ChemComm

FEATURE ARTICLE

Cite this: *Chem. Commun.*, 2024, **60**, 3891

Are nature's strategies the solutions to the rational design of low-melting, lipophilic ionic liquids?

John Yeboah,[a] Zachary J. Metott,[a] Christopher M. Butch,[a] Patrick C. Hillesheim *[b] and Arsalan Mirjafari *[a]

Ionic liquids (ILs) have emerged as a new class of materials, displaying a unique capability to self-assemble into micelles, liposomes, liquid crystals, and microemulsions. Despite evident interest, advancements in the controlled formation of amphiphilic ILs remain in the early stages. Taking inspiration from nature, we introduced the concept of lipid-like (or lipid-inspired) ILs more than a decade ago, aiming to create very low-melting, highly lipophilic ILs that are potentially bio-innocuous – a combination of attributes that is frequently antithetical but highly desirable from several application-specific standpoints. Lipid-like ILs are a subclass of functional organic liquid salts that include a range of lipidic side chains such as saturated, unsaturated, linear, branched, and thioether while retaining melting points below room temperature. It was observed in several homologous series of [$C_n$mim] ILs that elongation of *N*-appended alkyl chains to greater than seven carbons leads to a substantial increase in melting point (T_m) – which is the most characteristic feature of ILs. Accordingly, it is challenging to develop ILs with low T_m values while preserving their hydrophobicity and self-organizing properties. We found that two alternative T_m depressive approaches are useful. One of these is the replacement of the double bonds with thioether moieties in the alkyl chains, as detailed in several published papers detailing the chemistry of these ILs. Employing thiol–ene and thiol–yne click reactions is a facile, robust, and orthogonal method to overcome the challenges associated with the synthesis of alkyl thioether-functionalized ILs. The second approach involves replacing the double bonds with the cisoid cyclopropyl motif, mimicking the strategy used by certain organisms to modulate cell membrane fluidity. This discovery has the potential to greatly impact the utilization of lipid-like ILs in various applications, including gene delivery, lubricants, heat transfer fluids, and haloalkane separations, among others. This feature article presents a concise, historical overview, highlighting key findings from our work while offering speculation about the future trajectory of this *de novo* class of soft organic-ion materials.

Received 12th December 2023,
Accepted 19th February 2024

DOI: 10.1039/d3cc06066g

rsc.li/chemcomm

"If you want to understand function, study structure."
–Francis H. Crick, in What Mad Pursuit: A Personal View of Scientific Discovery (1988)

1. Introduction

Ionic liquids (ILs) have the potential to significantly transform the design of chemical processes and consumer products. Commonly recognized features defining ILs characterize them as a type of salt composed solely of ions, typically consisting of bulky organic cations and small organic or inorganic anions, exhibiting a melting point below 100 °C (although the latter prescription is arbitrary and not always practical when determining the classification of an IL).[1,2] Although the existence of low-melting molten salts has been known for some time, it has been only over the past three decades or so that they have been considered beyond academic curiosities. In recent times, ILs have become the subject of intense scientific scrutiny and industrial interest, as evidenced by notable publication rates and the introduction of ILs as both commercial products and commercialized IL-enabled processes.[1] Owing to the almost limitless range of ions that can be applied, ILs can provide alternative milieus with a considerably wider range of structures, properties, and functions compared to molecular solvents. In fact, the structural diversity and tunable characteristics of ILs have led to their recent establishment in commercial processes (ISOALKYL™ catalysts, biomass deconstruction, mercury capture) and products (GC column stationary phase, battery electrolytes).[3,4] Throughout this period, the scientific community

[a] *Department of Chemistry, State University of New York at Oswego, Oswego, New York 13126, USA. E-mail: arsalan.mirjafari@oswego.edu*
[b] *Department of Chemistry and Physics, Ave Maria University, Ave Maria, Florida, 34142, USA. E-mail: patrick.hillesheim@avemaria.edu*

has emphasized studying the physical characteristics of ILs – particularly their melting points (T_m) and miscibility (or lack thereof) with various molecular solvents. The field continually evolves with the emergence of new subtopics and research priorities that are adapted to incorporate fresh findings and discerning areas of applicability.

Much of the interest surrounding ILs arises from their role as alternative solvents, driven by their vanishingly low vapor pressures and molecular adaptability, predominantly attributed to their organic nature.[5] The vanishingly low pressure of ILs can be attributed to the robust interactions between their constituent ions in the liquid state, which result in high energy requirements for either a single ion or an ion pair to vaporize. A significant number of these ions consist entirely of organic structures. This unique feature allows chemists alike to leverage various synthetic strategies to modify the structure of the ions, tailoring the physicochemical properties of ILs. In fact, the ability to effectively tailor the physical, chemical, and biological properties of ILs through the manipulation of structure–property-function relationships forms the basis for the concept of "task-specific" ILs (or TSILs).[6] Beyond acting as simply non-volatile and unconventional solvents, TSILs are purposefully developed with a particular objective in mind. The term "task-specific" describes ILs whose structures have been tailored to achieve specific outcomes, *e.g.*, the enhanced solubility of a given species, catalytic activity, or a specific separation process.[6] However, one noteworthy physical property is conspicuously absent: ILs with nonpolar-like solvent properties.

John Yeboah

John Yeboah is an M.Sc. student under the supervision of Prof. Arsalan Mirjafari at the Chemistry Department of the State University of New York at Oswego. He works on designing synthetic lipid-like ionic liquids as effective gene delivery vectors. His primary goal is to understand the structure–property-function relationship and nanostructure of lipid-like ionic liquids using different experimental and theoretical techniques. He received his B.Sc. in Chemistry from the Kwame Nkrumah University of Science and Technology in Ghana, where he worked on assessing the antioxidant, antimicrobial and anti-inflammatory activities of secondary metabolites from purely cultured endophytic fungi, Fusarium culmorum.

Zachary J. Metott

Zachary Metott is an undergraduate student studying B.S. in Biochemistry at the Department of State University of New York at Oswego. He is currently working under Prof. Arsalan Mirjafari in his laboratory and began in April of 2023. Zachary's primary work is to develop lipid-like ionic liquids for their use as effective and safe gene delivery agents. With these new lipid-like ionic liquids, the relationship between structure, function, and property can be found through a combination of modular design, X-ray analysis, and computational modeling to rationalize the self-assembly and desired physicochemical and biological properties.

Christopher M. Butch

Christopher Butch is a master's student in Chemistry under the supervision of Prof. Arsalan Mirjafari at the Chemistry Department of the State University of New York at Oswego. His primary work is to develop synthetic lipid-like ionic liquids for energy-demanding applications, such as alternative fuel sources. With an interest in click-enabled synthesis, Christopher began his laboratory research in October 2023. He received his bachelor's degree in Chemistry from Le Moyne College in New York with a strong emphasis on Organic synthesis and Physical Chemistry.

Patrick C. Hillesheim

Patrick Hillesheim is an Assistant Professor of Chemistry at Ave Maria University in the Department of Chemistry and Physics. He earned his PhD, involving the structural analysis of chiral ligands for transition metal catalysts, at the University of Florida in 2010. He completed his postdoctoral training with Prof. Sheng Dai at Oak Ridge National Laboratory (2010–2013). His research interests are in ionic liquids, X-ray crystallography, non-covalent interactions, and supramolecular chemistry. Particularly, his research focuses on structural and energetic analysis of ionic liquids to unravel the correlation between the composition, interactions, and macroscopic behaviors of their constituent ions.

In contrast to most molecular liquids, ILs showcase a remarkable ability to self-assemble and form amphiphilic nanostructures.[7–10] That is, ILs exhibit nanostructural organization whereby microphase segregation results in the formation of polar (ionic) and nonpolar (alkyl) domains. Using molecular dynamics simulations, several groups demonstrated that these ILs have a complex, segregated nanostructure, particularly when the *n*-alkyl chains consist of four or more carbons.[11–13] Notably, Canongia, Lopes, and Pádua demonstrated that for longer chains ($C_n > 6$), the nonpolar alkyl domains become "continuous", resulting in the formation of self-assembled amphiphilic liquid systems.[13] A distinctive characteristic of ILs lies in their capacity to serve as a medium for surfactant self-organization into micelles, vesicles, lyotropic liquid crystals, and microemulsions. Crucially, amphiphilic ILs have intriguing features in terms of microheterogeneity stemming from the presence of charged ionic groups and nonpolar domains of cations. This nanoscale structural heterogeneity distinguishes ILs from molecular solvents as it generates hydrophilic and hydrophobic regions within the bulk IL structure that exhibit dual-solvent behavior. For example, an IL can incorporate a nonpolar solute in its nonpolar domains while simultaneously facilitating the dissolution of polar solutes through its hydrophilic domains.[14] Consequently, this unique property enables ILs to dissolve species with different nature simultaneously.

The formation of nonpolar domains in 1-*n*-alkyl-3-methylimidazolium-type ILs aligns coherently with the observation that an increase in chain length corresponds to increases in dependent physical properties in a manner analogous to the addition of CH_2 units in *n*-alkanes (*e.g.*, increased T_m, enthalpy of vaporization, heat capacity, entropy). This trend led Pádua and Lopes[15] to suggest that the alkyl chain exists in an "alkane-like environment." From a solvation perspective, ILs are commonly classified as polar or moderately polar,[16,17] primarily owing to their intrinsic ionic nature. Solvatochromism studies indicate that ILs lean toward the moderately polar end of the range.[18] Due to their polar nature, ILs readily dissolve moderately polar and polar solutes – "like-dissolves-like" rule – but often prove to be inefficient solvents for nonpolar compounds. This limitation restricts the applicability of ILs in chemical reactions and separation processes. To overcome this challenge, researchers have commonly opted to increase the length of the *n*-alkyl chain, thereby expanding the nonpolar domain. However, as illustrated in Fig. 1, this strategy significantly increases the T_m of the ILs due to increased non-covalent interactions (dispersion forces, H···H) between the nonpolar tails, producing ILs that are no longer liquid at room temperature. This escalation in fact places these T_m values above ambient levels and poses a challenge in designing ILs that are simultaneously low-melting yet capable of dissolving substantial amounts of lipophilic solutes, including those of biological origin, *e.g.*, fatty acids, steroids, and cholesterol.

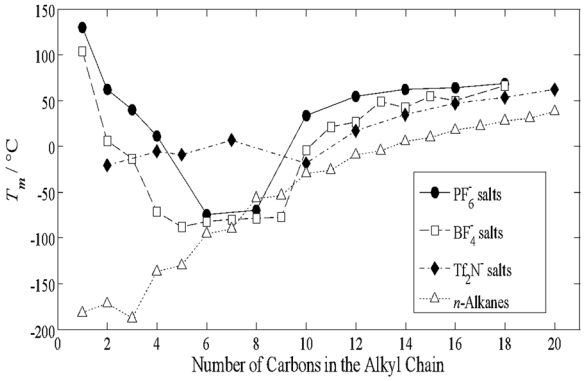

Fig. 1 Effect of alkyl-chain length on melting point (T_m) in 1-*n*-alkyl-3-methylimidazolium salts and corresponding *n*–alkanes. Reproduced from ref. 19 with permission from Jon Wiley and Sons.

Long alkyl chains causing an increase in T_m values are not restricted to ILs alone. In fact, it can also be observed in various biological molecules, and as usual, nature provides a solution for this phenomenon. The fluid mosaic model suggests that the phospholipid bilayer is a dynamic, two-dimensional solvent microenvironment, consisting of charged species with long aliphatic appendages.[20] The practical function of biomembranes is closely related to their fluidity, a property often quantified by reference to T_m – *viz.*, higher fluidity corresponds to lower T_m. The fluid mosaic model is evocative of nanoscale structuring ILs wherein distinct polar and nonpolar regions form. While the phospholipids often have a low T_m despite being composed of charged species with long aliphatic groups, the T_m of ILs generally, as noted, increases when progressively longer aliphatic appendages are used (*vide supra*).[21] The ability of cell membranes to maintain a high fluidity is attributed to homeoviscous adaptation (HVA). The lipid matrix in biological membranes can encompass saturated or unsaturated fatty acids, along with linear, branched, cycloalkylated, or functionalized (*e.g.*, hydroxylated or brominated) fatty acids. In HVA, it is commonly observed that organisms adapted to lower

Arsalan Mirjafari

Arsalan Mirjafari is Dr Richard S. Shineman Endowed Chair and Professor of Chemistry in the Chemistry Department of the State University of New York at Oswego (SUNY Oswego), a primarily undergraduate institution. His research centers on the click-enabled synthesis of novel functional ionic liquids with the overarching goal of uncovering specific molecular and biomaterial functions. This encompasses diverse applications, including vaccine preservation, gene delivery, lipid-like materials, and direct air capture of CO_2. He earned his PhD in Organic Chemistry from the University of Isfahan in 2009 and completed postdoctoral training with Prof. Jim Davis at the University of South Alabama (2010–2012).

temperatures have cell membranes with higher proportions of lipids containing unsaturated functional groups (particularly *cis* alkenes) like oleic acid or are otherwise "kinked" by the presence of alkyl branches, including mid-chain methyl and/or cyclopropyl groups (Fig. 3). The presence of these elements in the lipid chain reduces the packing efficiency of the hydrophobic components, leading to increased fluidity even at lower temperatures. Notably, the internal region of the lipid bilayer remains highly lipophilic despite the incorporation of these kinked elements. This combination of specific characteristics parallels the properties that we sought to integrate into ILs.

Given our group's interest in the rational design of ILs with tailored properties, we have embraced the opportunity to undertake this challenge: is there a way to design ILs with longer alkyl tails while manifesting low melting points? Drawing inspiration from nature's solutions to these questions (*vide infra*), we hypothesized that the strategic introduction of functional groups such as alkenes, thioethers, and cyclopropyl moieties into the long alkyl side chains would result in salts with nonpolar-like solvent properties yet exhibiting low T_m. Over the past decade, our research groups have dedicated extensive efforts to studying how structural modifications in the aliphatic chain structure impact the melting points of ILs, focusing primarily on the IL depicted in Fig. 2. These compounds have served as the workhorses of our research program since 2012. Our efforts in this regard have yielded significant achievements and helped establish relevant structural trends with respect to rational IL design.

It is worth mentioning that our studies primarily focused on the specific characteristics of *N*-bonded organic appendages attached to the cation. With respect to the anion, we prepared and studied salts of the bis(trifluoromethanesulfonyl)imide anion, $[CF_3–SO_2–N–SO_2–CF_3]^-$, denoted as NTf_2^- hereafter. This choice was based on the anion's inherent thermal, electrochemical, and hydrolytic stability as well as its ability to form sub-ambient melting ion pairs.[22] The NTf_2^- anion exhibits a high degree of charge delocalization and conformational freedom, making it possible to consistently produce ILs with low T_m.

In this feature article, our objective is to chronicle the origins of our experimental approach, summarize our discoveries, and outline our projections for the future development and utilization of this chemistry. It is important to clarify that our interests are expressly involved in the formation of lipophilic ILs, and not in amphiphilic compounds. This article only pinpoints the progress made in understanding and characterizing these lipophilic organic-ion materials with reduced T_m, and examples are primarily drawn from our work. For a comprehensive overview of amphiphilic ILs, we direct readers to reviews in the literature.[7–10,23–26] Additionally, for insights into nanostructures in protic ILs and deep eutectic solvents distinct from those discussed herein, we recommend the recent prospectives by Warr *et al.*[27]

2. Ene-bearing lipid-like ionic liquids

To establish whether an HVA-like effect can be exploited in the design of ILs, we embarked on the synthesis and phase behavior study of a series of ILs, each possessing a long alkyl appendage identical to that found in distinct, naturally

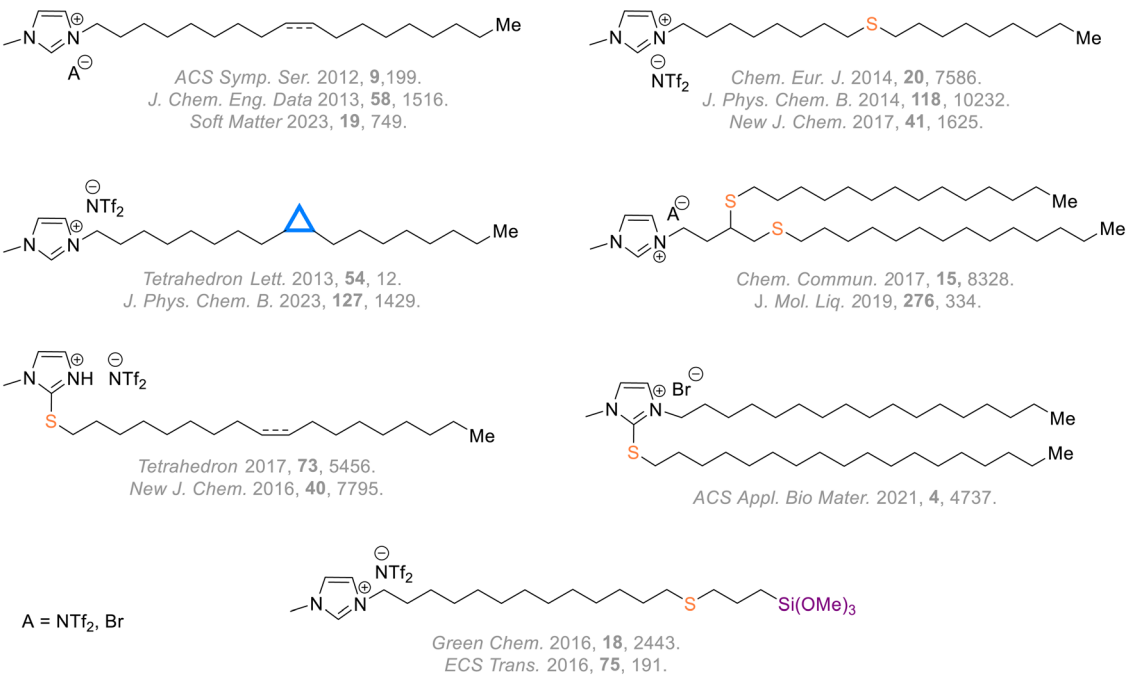

Fig. 2 Structures of cations comprising the ILs discussed in this work along with their corresponding publications. The most common anion in the structures of lipid-like ILs is bistriflimide, except where the ILs are designed for gene delivery applications. In these contexts, NTf_2^- is replaced with bromide due to its high toxicity.

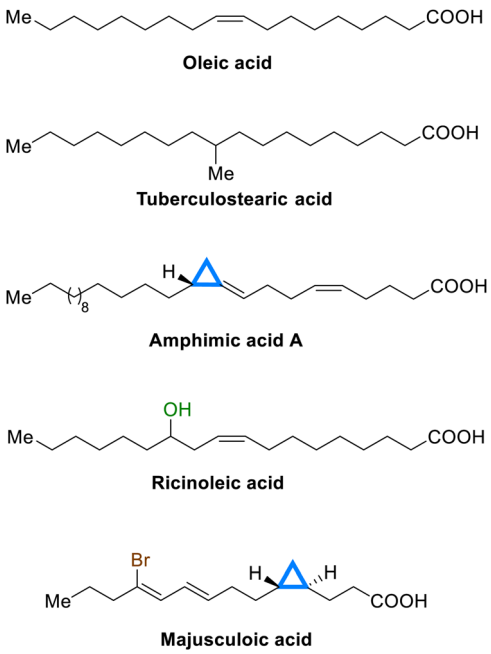

Fig. 3 Examples of naturally occurring fatty acids containing mid-chain motifs that induce structural kinking. Kinking is responsible for the T_m depression effect.

occurring fatty acid (Fig. 4). Similar to lipids, these ILs exhibit stepwise melting behavior that is characterized by thermotropic polymorphism. These compounds undergo solid–solid phase transitions towards disordered solid and/or liquid crystal phases prior to complete melting.[28]

To improve clarity and facilitate comparison to molecular analogs, a convention for differentiating the new ILs is employed. The compound number defines the base alkane or alkene chain and its unsaturation pattern is shown in Tables 1 and 2. The structures and T_m values of the parent series of saturated or unsaturated ILs (**-AL**), linear thioether-based (**-LT**), branched thioether-based ILs (**-BT**), cyclopropanated ILs (**-CP**), the analogous saturated/unsaturated fatty acid (**-FA**), and the methyl ester of the fatty acid (**-ME**) are depicted in Table 1. In addition, the ILs with fully saturated C_{16} (**1-AL**), C_{18} (**3-AL**), and C_{20} (**11-AL**) side chains and their T_m values provide baselines for comparison with the unsaturated variants of identical chain lengths as shown in Table 2. For instance, IL **5-AL**, the unsaturated counterpart of **1-AL**, is *cis*-unsaturated between C9 and C10. Likewise, **8-AL** are analogs of **3** that bear C18 side chains, *albeit* in which there is more than one double bond. These further differ based on the latter being either *cis*- or *trans*- in nature and in terms of their location along the C_{18} backbone.

In general, the cation of any IL has two main domains: the cationic moiety (*e.g.*, imidazolium, ammonium, phosphonium, *etc.*) and the ancillary alkyl chains. Rothenberg *et al.*[21] proposed that the former domain constitutes a symmetry-breaking region, the impact of which is eventually outweighed by the cumulative inter-chain dispersion forces of the progressively longer alkyl groups (Fig. 5). Modifications of the symmetry-breaking region such as branching, heteroatom substitution or alkyl chain length can profoundly impact the melting point of ILs by, in part, lowering the symmetry of the molecule as a whole. With these principles in mind, we sought the effective symmetry-breaking region of ILs through structural modifications of the alkyl chains.

Alkene moieties provide two readily accessible methods for controlling the T_m values for ILs: location and geometry. Remarkably, the mere inclusion of an alkene in the chain, whether *cis* or *trans*, substantially lowers the T_m values of the ILs. For example, $[C_{18}mim][NTf_2]$ has a T_m value of 53.5 °C. The addition of a *trans*-unsaturation at the C9 position lowers T_m to 16.0 °C (ΔT_m = 37.5).[28] In other studies, it was observed that increases in the dipole are inversely proportional to the melting point (*viz.*, higher dipoles lead to lower melting points).[33,34] The rationale behind the T_m depression with the *trans* alkenes is that increasing dipole moments increases cation–cation interactions, lowering T_m due to deceased cation–anion interactions. Thus, the increased dipole of *trans*-olefins and the resulting increase in local ordering of the cations may reduce the enthalpy of fusion (ΔH_{fus}), thus depressing the melting point.

Notably, incorporating a *cis* alkene has a more pronounced effect on fluidity, significantly lowering T_m compared to the saturated congeners. Introducing a *cis*-alkene kinks the chain, preventing efficient stacking (*viz.*, non-covalent interactions) of the alkyl chains, which hinders the formation of long-range order. The findings suggest that the addition of an unsaturated alkyl chain to the cation can also decrease the viscosity of ILs.[35] This "*cis*-kink" is, in a manner, analogous to the observed "crank-handle" conformation of saturated alkyl chains, which are observed in the solid state of related long-chained ILs.[36] However, while this crank-handle conformation is temporary, the *cis* alkene geometry remains constant, preventing the efficient formation of the alkyl-chain interactions.

Three important points of discussion should be addressed concerning the impact of the inclusion of alkene moieties: the tail length, locants, and the number of the *ene* moieties. First, the term tail here refers to the length of the alkyl chain after the double bond. Including a *cis* double bond always produced a lower T_m than the fully saturated congener, regardless of the overall length of the alkyl chain. Contrasting the alkyl chain lengths of the mono-unsaturated derivatives (**2-AL** *vs.* **5-AL**), we observe a modest increase in the melting points from −22.0 °C to −20.9 °C, respectively. When we compare the next related set of compounds (**6-AL** *vs.* **12-AL**), we see a more pronounced change in melting point as the alkyl chain increases: −9.8 °C to 4.2 °C. Speculatively, this could be due to the remaining alkyl tail reaching a critical point wherein stacking interactions from the tail begin to impact the thermophysical properties of the ILs. For **12-AL**, there is a remaining tail of eight carbons, which is right at the limit of the symmetry-breaking length discussed for alkyl derivatives, offering an explanation for the dramatically higher T_m of **12-AL** when contrasted with **6-AL**. However, further studies will be needed to grasp the structural pattern observed here fully.

Second, with respect to the location of the alkene, we demonstrated that lower T_m values in imidazolium-type ILs

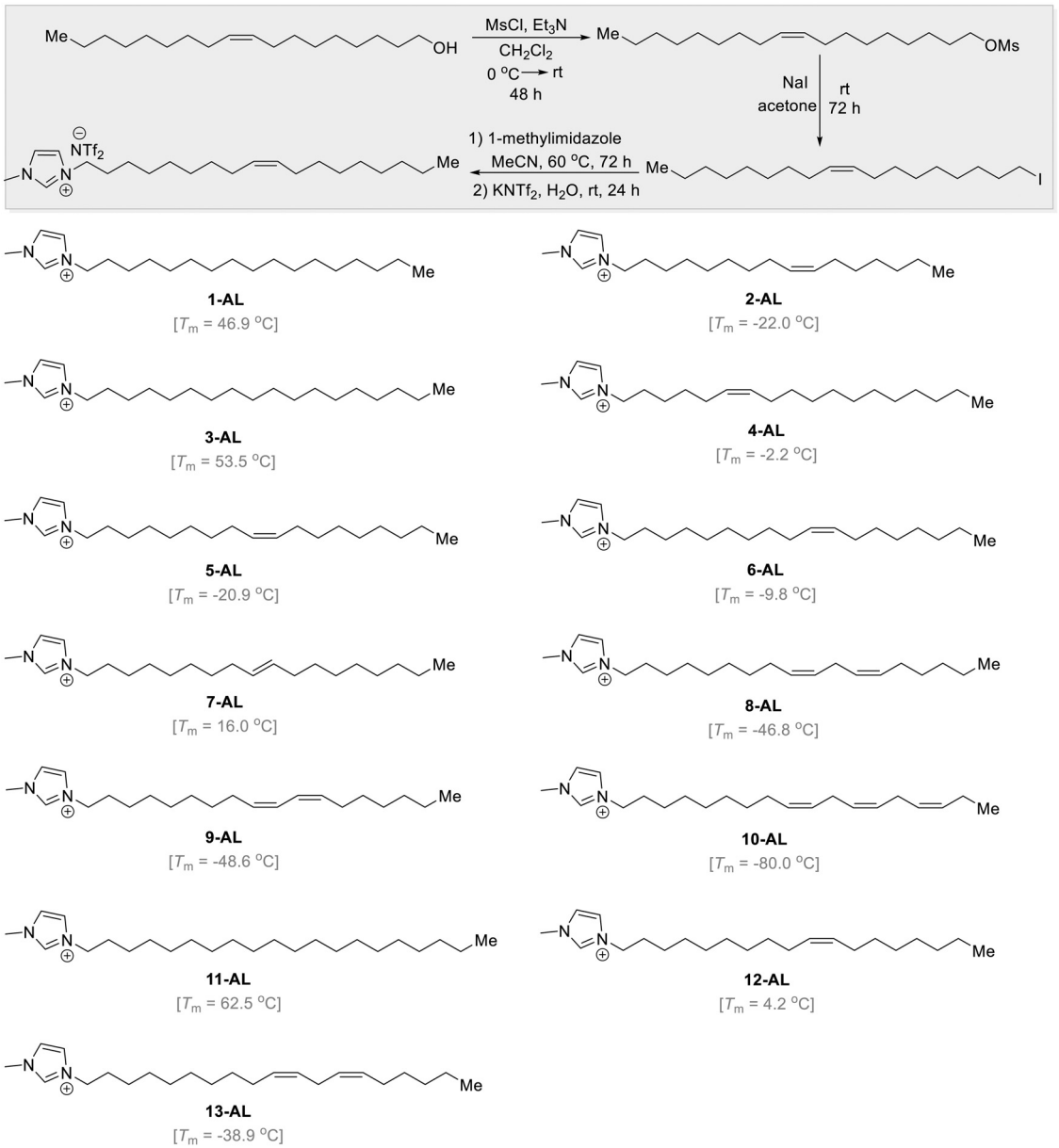

Fig. 4 The four-step synthesis and structures of the ene-bearing lipid-like ILs along with their T_m values (The counter anion is NTf_2^- that was omitted for clarity).[19,28] Each of the ILs has a long alkyl appendage identical to that in a natural fatty acid.

are observed regardless of whether the site of unsaturation was within the symmetry-breaking region or beyond it. However, *cis*-alkenes which are located within the established symmetry breaking region have a more pronounced impact on liquefaction behavior.[28] For example, T_m of the saturated $[C_{18}mim][NTf_2]$ is 53.5 °C. The inclusion of a *cis*-olefinic moiety at the C9 position of the chains (**5-AL**) reduces the melting point drastically, leading to a ΔT_m of 74.4 °C. Moving the double bond to the C11 position (**6-AL**) results in a melting point of −9.8 °C (ΔT_m = 63.3 °C). Thus, a modest change of two carbons in the positioning of the alkene results in an approximate 15% lowering of ΔT_m. However, the alkene at the C11 position lies outside the classically defined symmetry-breaking region and still produces a room-temperature IL with a melting point lower than that of its saturated counterpart.

West and coworkers studied the additional thermophysical properties of three $[C_{18}mim][NTf_2]$ ILs (**5-AL**, **7-AL**, **10-AL**), which were introduced to lower T_m compared to the saturated chain homolog (*vide supra*).[37] The temperature-dependent density, refractive index, and dynamic viscosity were all measured as functions of temperature at 1 bar and fit to appropriate model. The molar volume and volume expansivity were calculated from the density data. The slight structural variations, which led to notable differences in T_m values, have a far lesser effect on the liquid phase thermophysical properties of the ILs being investigated. The differences in density may arise from

Table 1 T_m values for saturated, *ene*-bearing, cyclopropanated ILs along with their fatty acid and methyl ester analogs. Reprinted from ref. 29 with permission from American Chemical Society

		T_m (°C)			
		Alkyl/alkenyl	Cyclopropanated	Fatty acid	Methyl ester
Base structure	Side chain	**-AL**	**-CP**	**-FA**	**-ME**
1	$C_{16:0}$	46.9	—	63.5	33.5
2	$C_{16:1}$, *cis* 9	−22.0	−35.0	0.5	−33.9
3	$C_{18:0}$	53.5	—	69.6	38.9
4	$C_{18:1}$, *cis* 6	−2.2	−1.5	29.8	—
5	$C_{18:1}$, *cis* 9	−20.9	−8.6	16.2	−19.6
6	$C_{18:1}$, *cis* 11	−9.8	8.3	12.0	−24.3
7	$C_{18:1}$, *trans* 9	16.0	21.2	43.7	10.3
8	$C_{18:2}$, *cis* 9, 12	−46.8	−27.7	−6.5	−35.0
9	$C_{18:2}$, *cis* 9, 11	−48.6	−25.5	22.0	—
10	$C_{18:3}$, *cis* 9, 12, 15	−80.0	−27.8	−11.0	—
11	$C_{20:0}$	62.5	—	75.5	54.0
12	$C_{20:1}$, *cis* 11	4.2	7.7	23.5	−34.0
13	$C_{20:2}$, *cis* 11, 14	−38.9	−7.5 (T_g)	—	—

Table 2 Comparison of T_m values for C_{16}, C_{18} and C_{20}-based ILs with functionalization at various locations within the aliphatic chain

Base structure	Chain length	Functionality	T_m (°C)
1-AL	$C_{16:0}$	—	46.9[19,28]
2-AL	$C_{16:1}$	Olefin, *cis* 9–10	−22.0[19,28]
2-CP	C_{16}	Cyclopropyl, *cis* 9–10	−35.0[30]
2-LT	C_{16}	Thioether, 9[*S*]	−2.8[29]
3-AL	$C_{18:0}$	—	53.5[19,28]
4-AL	$C_{18:1}$	Olefin, *cis* 6–7	−2.2[19,28]
4-CP	C_{18}	Cyclopropyl, *cis* 6–7	−1.5[30]
4-LT	C_{18}	Thioether, 6[*S*]	−11.3[29,31]
4-BT	C_{18}	Thioether, 6[*S*], 7-Me	−27.7[31]
5-AL	$C_{18:1}$	Olefin, *cis* 9–10	−20.9[19,28]
7-AL	$C_{18:1}$	Olefin, *trans* 9–10	16.0[19,28]
5-CP	C_{18}	Cyclopropyl, *cis* 9–10	−8.6[30,32]
7-CP	C_{18}	Cyclopropyl, *trans* 9–10	21.2[30]
7-LT	C_{18}	Thioether, 9[*S*]	24.5[29]
7-BT	C_{18}	Thioether 9[*S*], 10-Me	1.9[31]
6-AL	C_{18}	Olefin, *cis* 11–12	−9.8[19,28]
6-CP	C_{18}	Cyclopropyl, *cis* 11–12	8.3[30]
6-LT	C_{18}	Thioether, 11[*S*]	27.0[29,31]
11-AL	$C_{20:0}$	—	62.5[19,28]
12-AL	$C_{20:1}$	Olefin, *cis* 11–12	4.2[19,28]
12-CP	C_{20}	Cyclopropyl, *cis* 11–12	7.7[30]
12-LT	C_{20}	Thioether, 11[*S*]	22.5[29,31]

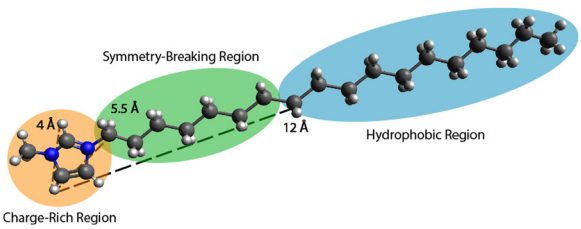

Fig. 5 Structural domains that determine the T_m values of imidazolium-based ILs. Reproduced from ref. 21 with permission from John Wiley and Sons.

variations in polarity between *cis* (**5-AL**) and *trans* (**7-AL**) isomers, while similar patterns can be observed in the trends of refractive indices. The viscosities of **5-AL** and **7-AL** were very similar, while **10-AL** exhibited a slightly reduced viscosity.

The T_m-lowering "alkene effect" of side-chain unsaturation is relevant not just when an IL headgroup is an imidazolium ring. Rather, it is operative across many classes of ILs, with their dramatically different headgroups and total organic content.[38] Surprisingly, the utilization of quaternary ammonium headgroups, with their more highly localized charge, appears to have little or no intrinsic T_m-increasing impact in these lipidic materials. Note that T_m of NTf_2^- salt of common gene transfection agent, DOTMA (1,2-di-*O*-octadecenyl-3-trimethylammonium propane chloride), with its two-side chain double bonds and quaternary ammonium headgroup is 6.4 °C higher than **9-AL**, with its two side-chain double bonds and more charge-diffuse imidazolium headgroup. This finding supports our hypothesis that the "alkene effect" is likely to have wide-ranging applications in formulating ILs. Furthermore, it suggests that incorporating double bonds into the structure of ILs can maintain low melting points while increasing the hydrocarbon side-chain content of the material.

Despite the clear benefits concerning the liquefaction of the ILs, introducing an alkene moiety does affect the chemical stability of the compounds. The olefinic ILs **2-AL**, **4–10 AL**, **12-AL**, and **13-AL** undergo discoloration over time when exposed to air. This suggests that these new species have high gas solubility (such as O_2), resembling the behavior of unsaturated fats like olive oil. Although the level of oxidation is not detectable by NMR within a month, the discoloration becomes noticeable visually, and the compounds develop a faint odor associated with side-chain oxidation products. While this reactivity may contribute to the biodegradability of the cations, it could be detrimental to many other applications. Therefore, controlling oxidation can be achieved by either storing the ILs under nitrogen or adding small amounts (approximately 1 mol %) of butylated hydroxytoluene (BHT), a common antioxidant in processed foods to prevent rancidity.[28]

To summarize, several key principles emerge regarding the inclusion of alkene moieties into ILs. First, unsaturation of the alkyl side-chain results in a lowering of the melting point, whether in *trans* or *cis* diastereomers. In the present examples,

the inclusion of *cis* double bonds in the side chains is the more powerful downward driver of T_m. Second, the alkene location drastically impacts the compounds' thermophysical properties. Including the alkene within the classically defined symmetry-breaking region of the side alkyl chain ($C_n \lessapprox 8$) has a more significant impact on the ΔT_m than alkenes outside of this region. Finally, the inclusion of multiple alkene motifs further decreases the melting points of the ILs, with the diene-bearing IL C_{18}:3[9,12,15] (**10-AL**), showing the lowest T_m of the currently examined lipid-like ILs (Table 1).

3. Thioether-functionalized lipid-like ionic liquids

''*The ideal chemical process is that which a one-armed operator can perform by pouring the reactants into a bathtub and collecting pure product from the drain hole*''.

–Sir John Cornforth, Chemistry in Britain, 1975, 432.

While incorporating unsaturation into aliphatic chains of the imidazolium cations significantly lowers the melting temperatures of ILs compared to their saturated counterparts, it also makes the ILs more susceptible to chemical degradation. Consequently, we set out to identify a scission-resistant ''effect isostere'' capable of lowering the melting temperature of lipid-like ILs, while preserving their lipophilic nature but without the coincident air sensitivity. Our research groups have discovered that incorporation of sulfur into alkane chains leads to a *gauche* conformation of the chain due to their larger size and the presence of the non-bonding electron pairs. These distinctive properties of thioether groups allow them to effectively act as a kink in the chain resulting in a lower T_m. Over the past decade, we have reported significant success in exploiting this phenomenon to develop lipidic ILs that combine low T_m values with improved oxidative stability compared to lipid-like ILs with unsaturated side chains.

Incorporating a thioether functionality within an IL required a new synthetic approach compared to the alkenes. Furthermore, with the eventual hopes of generating functional materials for industrial applications, we also sought to maintain a high atom economy within the synthesis. Thus, we pursued click chemistry as part of the synthetic route for these ILs. Generally, the fundamental principle of click chemistry is to synthesize and identify functional molecules efficiently.[39] This paradigm has much to offer for the effective synthesis of novel functional cations of IL synthesis, especially for the post-quaternization synthetic schemes.[40] In fact, since the functionalities in task-specific ILs are frequently heteroatom-based, their preparations demand strategic planning to prevent the formation of undesired byproducts from competing side reactions.[6] Therefore, methods that focus on constructing target molecules through orthogonal reactions are highly valuable in this field. Drawing inspiration from the structural principles gleaned from the alkene studies, we employed thiol–X (X = ene and yne)[41] chemistry to synthesize a series of thioether-functionalized ILs in excellent yields and in a remarkably short period of time (roughly a library of 100 task-specific ILs). These photoclick reactions enabled us to strategically incorporate thioether functionality into ILs' side chains, leading to significant control over the liquefaction behavior of the lipid-like ILs.[29,31,42–47]

The inclusion of a thioether moiety within an alkyl chain imparts significant molecular asymmetry due to two notable properties of the thioether motif. First, the relative energy levels of the *gauche* and *anti* conformations of C–S–C bonds differ by only *ca.* 0.1 kcal mol^{-1}. Second, the barrier of rotation for the thioether moieties is lower than that of alkyl or ether moieties. These two features are key in rationalizing the low melting points for thioether functionalized ILs. For long-chain ILs multiple readily accessible conformations and low barriers to rotation prevent the stacking of alkyl chains and thus hinder the efficient formation of alkyl–alkyl interactions, leading to solidification of the IL (*i.e.*, freezing/crystallization).

In a manner analogous to that observed with alkenes, the positioning of the sulfur group allows for the shaping of thermal properties. Fig. 6 and Table 2 succinctly summarize the T_m values of a series of linear thioether-based ILs with varying sulfur positions in the alkyl chain. Several observations are made when examining the data in T_m of the compounds. First, the overall lowest T_m values (minima) for the compounds are all within ~ 1 °C (*ca.* −24 °C) despite the changes in sulfur position and the tail length. Of note, the compound with a C_{16} equivalent chain bearing a sulfur atom at the C5 position exhibits the lowest T_m at −24.9 °C. Second, a clear relationship exists between the sulfur position, the alkyl chain length, and T_m. Specifically, the lowest T_m values for C_{16}, C_{18}, and C_{20} occur when the sulfur is at C3, C5, and C7 positions, respectively. Thus, as the alkyl chain length increases by two CH_2 moieties, the optimal sulfur position also shifts (optimal simply implying the lowest T_m). Notably, the external alkyl chain beyond the sulfur moiety is equivalent in these compounds with 13 remaining carbons. While admittedly speculative, it has been shown that odd-numbered alkyl chains lead to lower melting points, whether in ILs or simple *n*-alkanes. Thus, perhaps the outside alkyl chain length being an odd number helps similarly lower the melting points.

Third, all sulfur positions leading to the lowest T_m values are within the established symmetry-breaking domain of the ILs. This observation aligns with principles established in many studies of these long-chained ILs about the impact of different regions of the chains (symmetry-breaking *vs.* hydrophobic). Finally, the range of T_m tracks with increasing chain length with the compounds following the expected relationships of increasing alkyl chain length and increasing T_m due to the collateral increase in inter-side chain non-covalent interactions.

From the data gathered, we observed that strategically placed sulfur atoms as thioether linkages in lipidic compounds result in a noticeable decrease in their melting points. However, this decrease is less significant than that caused by unsaturation when contrasting the saturated and unsaturated reference compounds. The decrease in T_m observed for these single *S*-atom replacements was significant, ranging from a ΔT_m of 45% to 72% of the depressive effect caused by the olefin

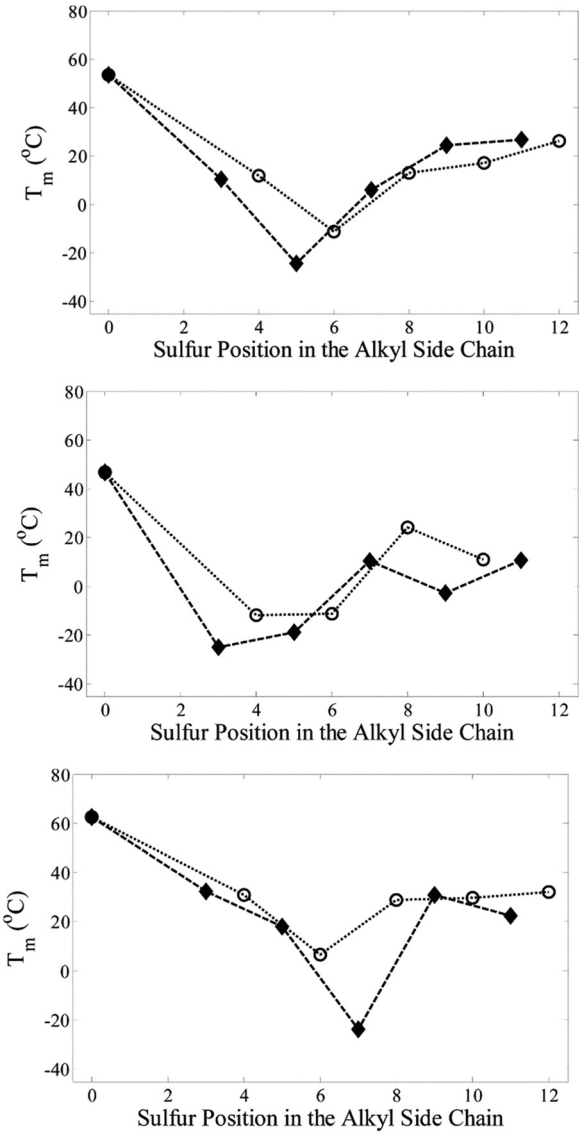

Fig. 6 T_m values of the 1-thiaalkyl-3-methylimidazolium-based ILs with an equivalent chain length of C16 (top), C18 (middle) and C20 (bottom) as a function of the position of the sulfur in the chain. The odd (♦)/even (○) sulfur positions have been plotted separately to help distinguish trends. Reprinted from ref. 29 with permission from the American Chemical Society.

module. It is noteworthy that this phenomenon is applicable in fatty acids also, indicating its versatility as a tool for engineering T_m and potentially other fluid properties such as viscosity in lipidic soft materials.

Having established several vital trends with respect to thioether moieties, we began to examine the effects of branching on T_m of ILs, combining the electronic impact of thioethers with sterics.[31] There is considerable structural latitude possible when designing highly lipophilic ILs that demonstrate low T_m values due to cumulative disruptive effects of thioether and branching on packing efficiency. Notably, organisms often utilize lipid branching to depress T_m and modulate cell membrane fluidity.[48] We synthesized a series of branched imidazolium-based ILs with thioether alkyl chains *via* the thiol–ene reaction (Scheme 1).

Controlled by the solvent polarity, the unusual predominant Markovnikov-oriented addition of sulfur across the double bond was observed, leading to the formation of branched ILs (**-BT**) with lower T_m compared to their linear counterparts (Table 2). Several important structural details emerge when examining the trends in T_m for these compounds. First, the branched ILs, whether internal or external, exhibit the lowest T_m values at −27.7 °C. Second, the lowest T_m occurs when methyl groups are located within the classically defined symmetry-breaking region (**4-BT**). Third, an interesting pattern emerges when comparing the changes in T_m between the linear and external methylated ILs. The difference in T_m values for the positionally substituted thioether motifs (**4-LT** *vs.* **4-BT**) reveals a predictable increase in T_m as the methyl group shifts away from the imidazolium core. Specifically, the difference in T_m values for 6[*S*], 8[*S*], and 9[*S*] compounds shows ΔT_m of 16.4 °C, 19.4 °C, and 22.6 °C, respectively. An increase of *ca.* 3 °C ΔT_m for these sequential compounds is noted. While the exact nature of this 'pattern' is yet unknown, these compounds stand out by virtue of this direct pattern.

Furthermore, we used the thiol–yne reaction to construct task-specific ILs that are useful for DNA complexing as gene transfection agents.[45] The addition of RS$^\bullet$ and H$^\bullet$ radicals to *yne*-bearing ILs incorporates two new thioether moieties which move the position of the hydrophobic/hydrophilic interface closer to the polar headgroups, extending the hydrophobic domain (Fig. 7). As noted in an earlier study,[31] we developed compelling evidence that the incorporation of branches in the long, lipidic side-chains of imidazolium-type thioether-based ILs brings about a dramatic reduction in T_m *versus* saturated analogs with side chains of the same length (*vide supra*). Remarkably, the thioether side chains in these ILs exhibited a branched arrangement with respect to each other, while those in the ILs with the fully saturated side chains (**1-AL** and **3-AL**) projected from the cationic locus in a symmetrical, parallel manner. The introduction of two sulfur atoms in the side chains of these new salts significantly lowers T_m despite a doubling of the alkyl content and potentially increased intercation dispersive attractions compared to the reference ILs. This again supports the proposition that when incorporated into ILs, thioether side chains pack less densely than those that are fully saturated, likely because of the cumulative effect of the chain kinks, along with its less-dipolar headgroup-linker domain, compared to ethers and esters. The effect on T_m wrought by the position of the thioether branches in the long aliphatic side chains is particularly noteworthy. Predictably, the sulfur atoms and branching features in the lipid chains of these ILs imbue it with a much lower T_m because the thioether branch is located in the symmetry-breaking area of the cation.

To further advance this class of ILs, we reported the development of new ILs, utilizing the combined effects of unsaturation and sulfur modules. Our primary objective was to create IL platforms featuring both *cis*-olefinic and thioether groups in the side chain, enhancing their fluidity by reducing T_m compared to their counterparts with mid-chain thioether groups. In doing so, we developed new thioether-bearing ILs through the systematic variations at the nucleophilic sites (*S*- and/or

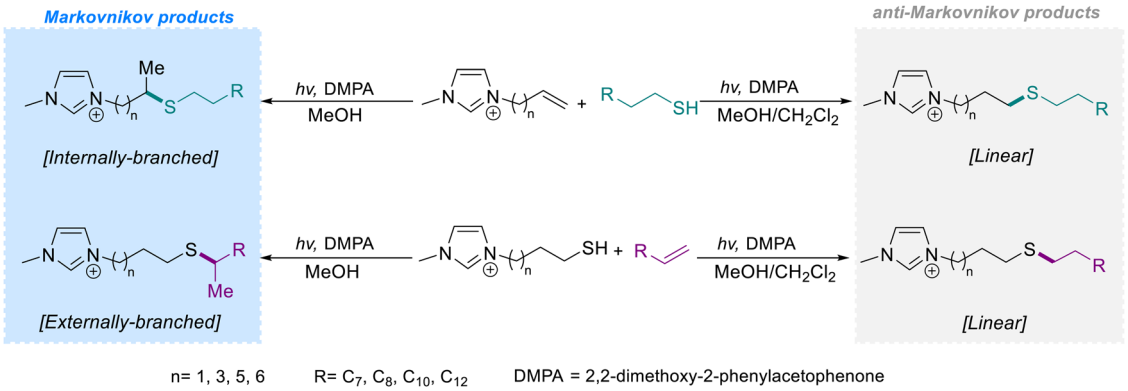

Scheme 1 Formation of linear and branched thioether-based lipid-like ILs *via* thiol–ene click chemistry.

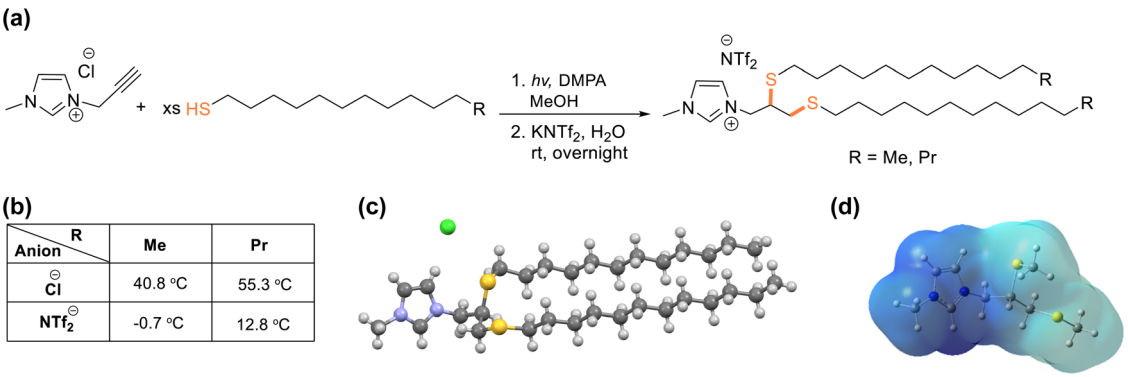

Anion \ R	Me	Pr
Cl^-	40.8 °C	55.3 °C
NTf_2^-	-0.7 °C	12.8 °C

Fig. 7 (a) Synthesis of the thioether-based ILs using the thiol–yne reaction. (b) Comparison of T_m of the ILs paired with Cl^- and NTf_2^- anions with an equivalent chain length of C_{16} and C_{18}. (c) Crystal structure of the thioether-based lipidic IL with chloride anion and C16 tails. (d) The electrostatic potential energy map of the thioether-based imidazolium cation. The boundary between hydrophilic/hydrophobic domains can be clearly observed, showing that sulfur atoms are located in the hydrophobic domain. Reprinted with from ref. 45, 46 with permission from the Royal Society of Chemistry and Elsevier.

N-substitution) of 2-mercapto-1-methylimidazole (commonly referred to as methimazole)[49] as a planar, chemically robust, and electron-deficient aromatic heterocycle with widespread applications in medicinal[50] and coordination[51] chemistry.

We consecutively developed a series of monosubstituted methimazolium-based ILs containing long saturated and *cis*-unsaturated C_{16}–C_{20} alkyl appendages with low T_m values *via* the *S*-alkylation of methimazole (Fig. 8).[49,52] The comparative T_m values of the new ILs and corresponding references clearly demonstrate the remarkable impact of unsaturation and the secondary effect that is rooted in the presence of sulfur in the chain (Fig. 8). Of note, single-crystal data from one of the compounds indicated that the S–$C_{(ring)}$ bonds (1.736 Å) are shorter than the regular C–S bond (1.763 Å), rationalized by the charge delocalization between the ring and the sulfur atom (Fig. 8b). Remarkably, this leads to an enhancement in the long-term oxidative stability of the ILs relative to thioether-type ILs. As confirmation, attempts to oxidize the sulfur atom to sulfoxides/sulfones were unsuccessful. An important axiom in the IL design suggests that more charge-diffused ions tend to lower the T_m values of resulting salts.[53]

In conclusion, our studies of thioether functionalities incorporated into long-chained ILs reveal several notable structural principles. First, thioethers function similarly to alkenes in that the inclusion of these sulfur groups lowers the melting point of ILs. However, the mechanism in which thioethers accomplish this is more complex than for alkenes by allowing access to multiple, energetically accessible conformations in which the alkyl chains are kinked, thus preventing stacking. Second, branched thioethers offer an exceptionally versatile toolbox of sterics and electronics concerning the development of low-melting ILs. Finally, the thioethers increase the chemical stability of the ILs when compared to their olefin-bearing congeners.

4. Cyclopropanated lipid-like ionic liquids

"*Reactivity isn't everything; it's the only thing*"

– K. B. Sharpless, 15th National Meeting on Fluorine Chemistry, Shanghai Institute of Organic Chemistry, Nov. 2018.

As discussed previously, the inclusion of side chain unsaturation affects the chemical stability of ILs, making them more susceptible to oxidative degradation. Likewise, thioethers can undergo aerobic oxidation to sulfoxides, *albeit* slowly, although

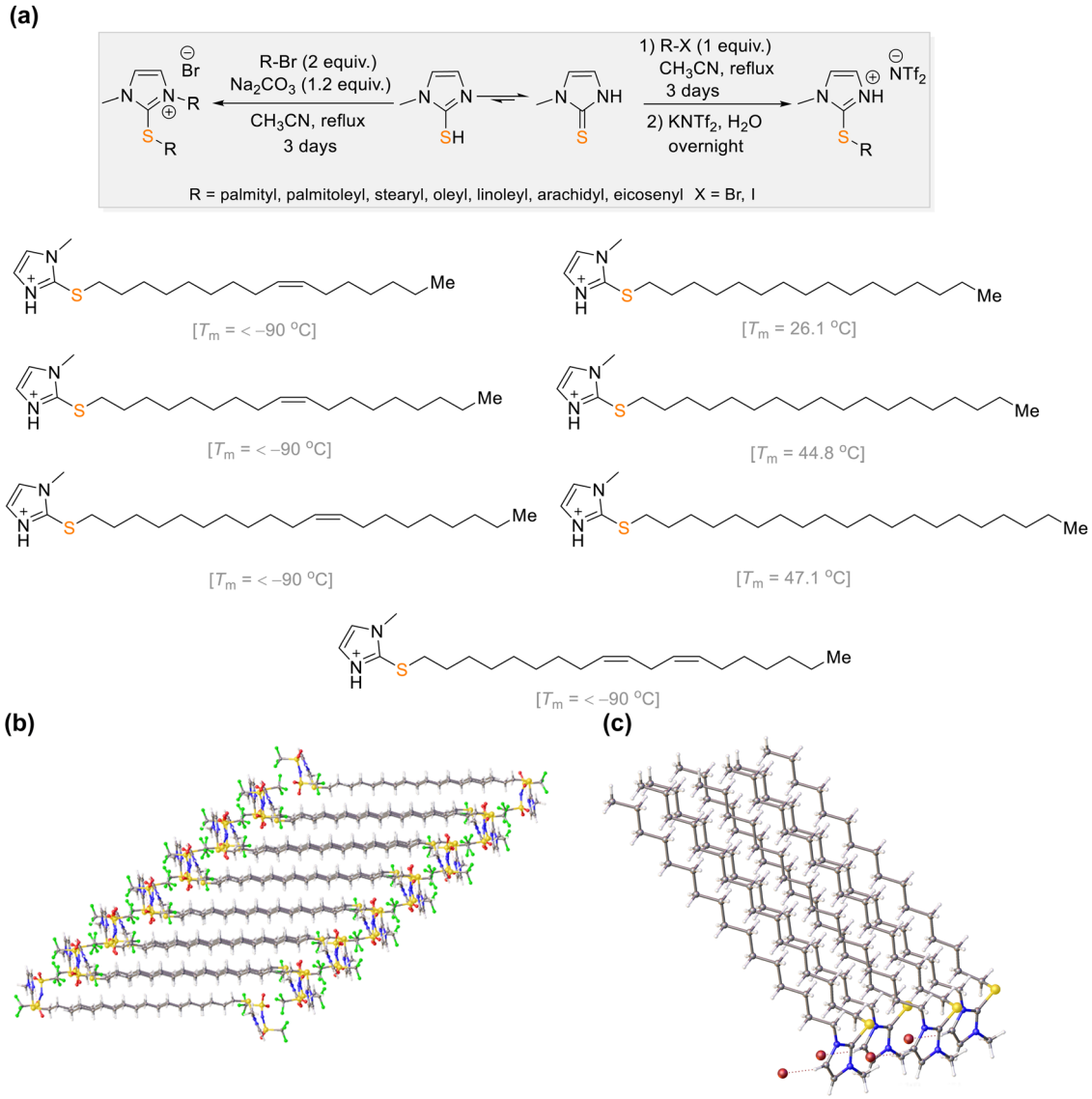

Fig. 8 (a) Synthesis (top) and structures (bottom) of the lipid-like ILs constructed through the *S*-alkylation and *N*,*S*-dialkylation of the methimazole heterocycle, along with their T_m values. Methimazole exists in equilibrium between the 2-thione and 2-thiol tautomeric forms. The NTf_2^- anion was omitted for clarity. (b) and (c) the packing diagrams of mono- and dialkylated methimazolium-based ILs, respectively. The molecules were found to self-organize *via* distinct noncovalent interactions, including coulomb and van der Waals forces and form an interdigitated bilayer-structure with a clear segregation of polar and nonpolar domains. Reprinted with from ref. 49, 54 with permission from the Royal Society of Chemistry and American Chemical Society.

this oxidation process typically does not result in molecular cleavage. Thus, we continued to seek alternative T_m depression approaches that maintain a similar geometry while increasing the chemical stability of the alkyl chains. As with the alkene groups, nature provides a source of inspiration, as certain organisms employ cyclopropyl moieties as a motif to regulate the fluid properties of the cell membranes in various natural fatty acids and natural products (Fig. 3).[55,56] For example, cyclopropanated fatty acids are prevalent in *Escherichia coli*, *Streptococcus*, and *Salmonella*, where these compounds are produced by *in situ* methylation of the double bond in the corresponding *cis*-unsaturated fatty acids.[57] In addition, it was reported that cyclopropanated mycolic acids in the cell membranes of *M. Tuberculosis* decrease the fluidity, thereby reducing their permeability to potentially toxic compounds and certain antibiotics.[58,59]

Several recent reports have found applications for cyclopropane-bearing ILs. For example, due to intrinsic ring strain, cyclopropane is a desirable structural component for creating high-energy fuels for energy-demanding applications such as long-haul transport, aviation, and rocketry.[60] In fact, high-angle straining of the cyclopropyl bonds causes an increase in the fuels' net heat of combustion. In addition to showing promise in numerous applications, monocyclopropanated IL **6-CP** demonstrated superior thermal stability compared to other lipid-like ILs tested, including **1-AL**, **2-AL**, **5-AL**, **6-AL**, **7–AL**, and **8-AL**.

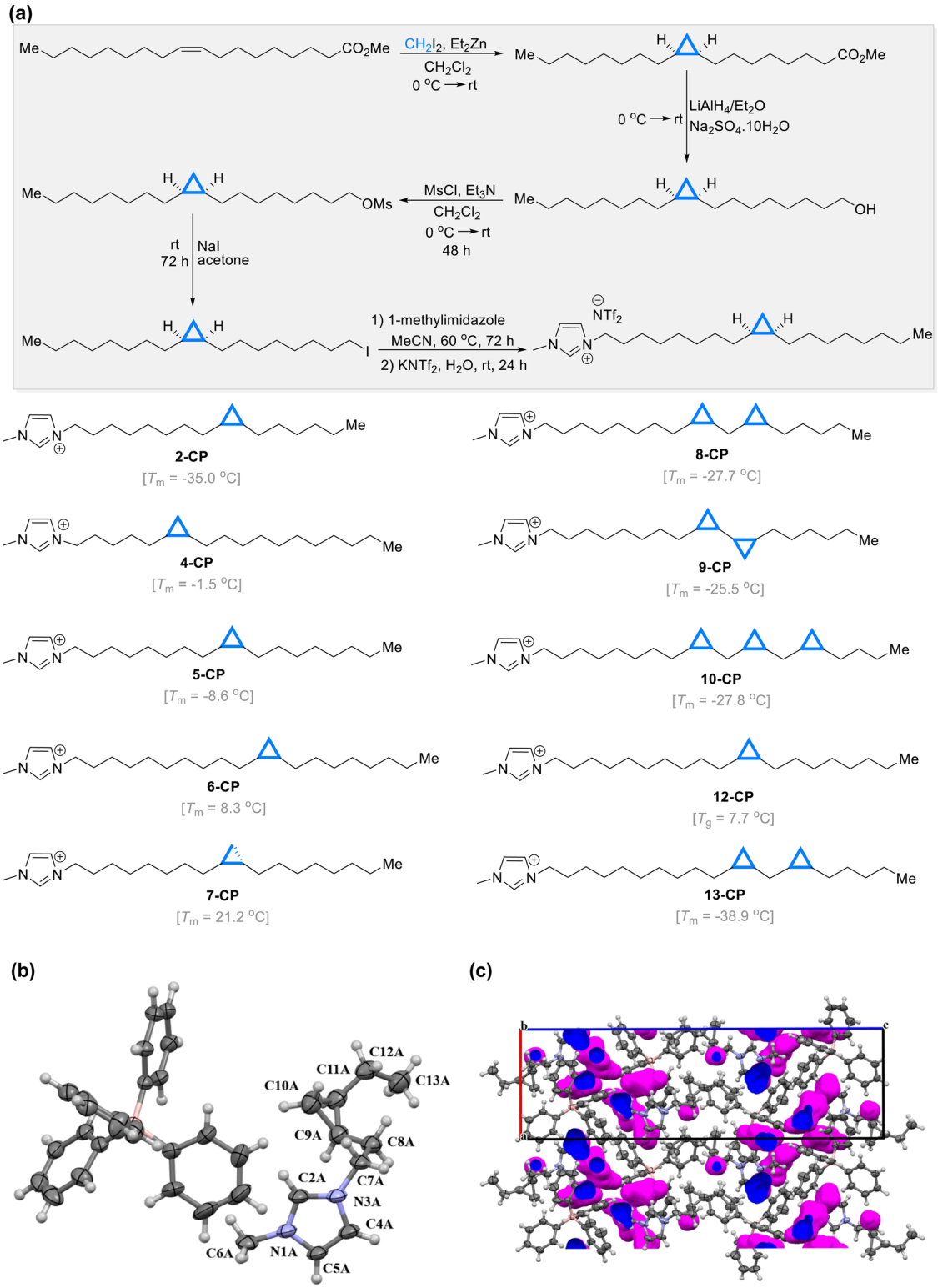

Fig. 9 (a) Top: Six-step synthesis of **5-CP** as a representative method for the synthesis of cyclopropanated ILs. Bottom: Structures of synthesized cyclopropanated ILs with their T_m values. The NTf_2^- anion was omitted for clarity. (b) Asymmetric unit of a cyclopropanated salt with the C_6 side chain, paired with Ph_4B^- anion, that was suitably single-crystalline at room temperature. Since we were not able to isolate a cyclopropanated IL in single-crystalline form, we synthesized a imidazolium-based cyclopropanated salt with a significantly shorter-chained counterpart. (c) Depiction of the void space within the crystal structure. Reprinted with from ref. 30 with permission from the American Chemical Society.

Inspired by these findings, we synthesized a series of ten mono- and polycyclopropanated ILs in a six-step process (Fig. 9a).[30,32] We hypothesized that incorporating cyclopropanated fatty acids in the design of lipid-like ILs can provide valuable information on structural elements that achieve both low-temperature fluidity and high lipophilicity. In order to maximize fluidity, we strategically incorporated the cyclopropyl group at the specific "nature-selected" C9–C10 or C11–C12 positions in several ILs such as **5-CP**, **6-CP**, or **9-CP** (Fig. 9). Furthermore, we thoroughly examined the impact of cyclopropanation on the thermophysical properties of these ILs to understand the optimal placement of the cyclopropyl group to achieve the highest possible level of fluidity. We observed that ILs with long alkyl appendages responded to side-chain cyclopropanation in a manner that mimicked the mechanisms underlying HVA in living organisms (Tables 1 and 2).

One observed trend is that the T_m values of the ILs increase as they are converted from unsaturated to cyclopropanated species, with the extent of cyclopropanation playing a role in this increase. Analogous to an alkene moiety, a cyclopropyl ring imparts rigid geometric constraints on the alkyl chain into which it is embedded. Specifically, both *cis* and *trans* forms of the rings are possible, with either isomer changing the local geometry surrounding the ring. Thus, the expected melting point depression associated with the inclusion of this chain-kink was observed in long-chain ILs containing *cis*-cyclopropyl moieties as part of their design. For instance, comparison of the saturated alkane **3-AL** with the cyclopropanated analog **5-CP** resulted in a ΔT_m of 62.1 °C. This change in melting point is primarily attributed to the conformation of the alkyl chain due to the *cis* cyclopropyl ring. Moreover, the inclusion of multiple rings in the alkyl chain further lowers melting points. For example, the inclusion of two cyclopropyl rings in the C_{18} chain at the C9–10 and C11–C12 positions lowers the melting point of **8-CP** to −27.7 °C, making polycyclopropanated alkyl chains a viable option for further tailoring the properties of lipid-like ILs.

On average, there is an 8.0 °C increase in T_m when converting from single *cis* unsaturation to single *cis* cyclopropanation. An approximate 25 °C increase in T_m is observed for double cyclopropanation compared to doubly unsaturated species and up to a 52 °C increase for tri-unsaturated species (Table 1). This suggests that cyclopropanation restricts chain mobility in the liquid phase by reducing the degrees of freedom and limiting entropy, resulting in decreased enthalpy of fusion and higher T_m values. However, it is worth mentioning that the cyclopropyl moieties still result in T_m depression when compared to their saturated analogs while boasting higher thermal and chemical stability than their unsaturated counterparts. A similar trend in physicochemical properties is observed for cyclopropanated fatty acids (Table 1).

We further contrasted several C_{18}-based ILs with variations at the C9–C10 position of the aliphatic side chain as shown in Fig. 10. The most valuable insight to be drawn from the present study is well demonstrated by the following: the saturated IL (**2-AL**) has a T_m value of 53.5 °C, while its olefinic counterparts gave T_m values of −20.9 °C for the *cis* (**5-AL**) and 16.0 °C for the *trans* (**7-AL**) isomers, providing melting point differences of 74.4 °C and 37.5 °C, respectively. As demonstrated in Fig. 10, the influence of a "kink" in the aliphatic side chain plays a crucial role in the packing efficiency of the lipidic molecules and the subsequent T_m values. In addition, introducing a thioether bond at the C9 position of the C_{18} chain led (**7-LT**) to a melting temperature of 24.5 °C, similar to **7-CP** with *trans* cyclopropanated structure (T_m = 21.2 °C). Cyclopropane ring acts as a chain-kink agent, mimicking the geometric environment of both alkene and thioether moieties. Specifically, as observed through crystallographic studies, the inclusion of the cyclopropane ring frustrates efficient chain packing. Second, the cyclopropanated moieties display higher chemical stability when compared with either the alkene or thioether moieties. Furthermore, the inclusion of the strained ring system expands the potential energy-demanding applications (*e.g.*, fuels for aviation and rocketry). Finally, adding multiple rings in key locants in the alkyl chains results in lower melting points than mono-cyclopropanted systems. We theorize this effect is simply a compounding result of our overall "liquefaction" theory: prevent/hinder alkyl interactions to lower melting points.

5. Crystallographic studies of lipid-like ILs

In our research on ILs, we focused on controlling physicochemical changes by modifying the cationic alkyl structure.

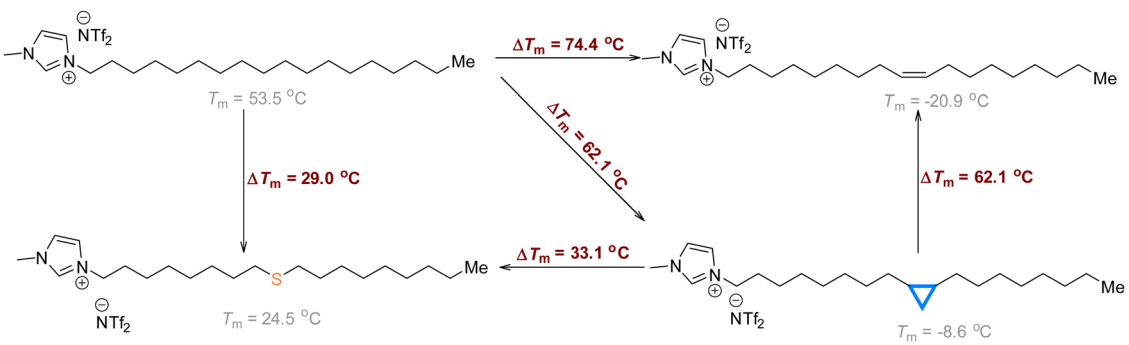

Fig. 10 Comparative ΔT_m values among three generations of lipid-like C_{18}-based ILs.

The question then turns to how we can explain and rationalize the observed trends in the melting points of ILs. Moreover, can we control or break these expected trends? This was, and is, a critical question that drives our research. There are various methods in which one can study the structure of ILs, including infrared and Raman spectroscopy,[61] nuclear magnetic resonance,[62] and theoretical computational studies.[63] There exist further methods, of course, and the examples presented herein are just a minuscule sampling meant to whet the appetite and provide any reader, who is so inclined, to pursue additional sources. A point to keep in mind is that the field of ILs always provides a wealth of interesting results and opportunities to study the unexpected properties for those willing to branch out to discover the limitless potential of these materials such as studying acoustic properties of ILs.[64]

For our work, we incorporated crystallography as a way to understand the structure, long-range ordering, and non-covalent interactions present within ILs. Crystallography has a storied history throughout the physical sciences.[65] Examining the solid-state crystalline structure of compounds has helped establish countless scientific principles throughout the past century.[66] The field of ILs has likewise benefited from crystallography, with many fundamental concepts of structural IL chemistry being discovered through the intentional use of single-crystal X-ray diffraction. In fact, the first paper on modern ILs reported several crystal structures of imidazolium-based compounds.[67] Since this seminal paper, there have been numerous crystallographic studies[68] that have examined key concepts in the field of ILs, such as polymorphism and its relation to melting points,[69] as well as the importance of conformational freedom of alkyl chains.[70]

There is an important idea to bear in mind with respect to the crystallographic studies of ILs: ILs are typically designed to frustrate crystallization, thus significantly complicating crystallographic studies. To borrow a phrase from Professor Anja-Verena Mudring at Aarhus University: "*Solidification and especially crystallization of ILs is by no means an easy task…*"[71] Indeed, we have found this statement to be true countless times. However, despite the challenges of studying ILs using crystallography, this technique has proven to be of fundamental importance to our work and many other groups in driving the rational development of structural principles of amphiphilic ILs.

ILs are cybotactic, possessing a measure of short-range order in the liquid state.[72] This ordering is influenced and controlled by the intermolecular forces present in the molecules in question. For example, the H-bonding capacity of water results in the formation of localized structure which can extend for several angstroms.[73] Likewise, ILs in the liquid state possess short-range order, which is dictated, to an extent, by the composition of the ILs (*i.e.*, cation structure, alkyl chain length, anion).[74] Two important ideas should be explicitly stated. First, local ordering is dynamic with ordered regions in flux as expected with free-flowing liquids. Second, the electrostatic charges in ILs are dominant forces. The non-covalent interactions, however, are not unimportant or to be dismissed with respect to their impact on IL structure and properties. The point remains that the local ordering of ILs in their liquid state is influenced by non-covalent interactions, *e.g.*, H-bonds, π-stacking, σ-holes, and so on. Crystallography provides key insight into the presence, absence, and preference for these interactions.[75] It follows that knowing the interactions in the crystalline state can give an understanding of the solution and liquid states of the ILs, allowing for rationalization of the physicochemical behavior of the compounds.[76,77]

Seeking more significant insights into the structure–fluidity correlation, we conducted crystallographic studies of a representative saturated IL to gain deeper insight into the nature of the structure and the impact on the packing and chain order. A series of ILs bearing saturated hexadecyl alkyl chains were synthesized and characterized *via* single-crystal X-ray diffraction. As noted, one of the challenges with the crystallography of ILs is that these systems are, in many ways, designed to frustrate crystallization, a form of anti-crystal engineering.[78] However, it has been well established that 1,2-dimethylimidazolium-based ILs ([$C_n$dmim]) possess higher melting points and, typically, higher crystallinity. Leveraging this property, three crystals of the [C_{16}dmim] cation were grown with a Br^-, I^-, and NTf_2^- anion.[79] It should be noted that the Cl^- bearing compound was crystalline, although single crystals suitable for diffraction could not be isolated. The three crystals provided a wealth of knowledge concerning the structure of the cation, the non-covalent interactions present, and how the varying anions affect these interactions. Moreover, careful examination of these three crystals, coupled with Hirshfeld surface analysis, provides an essential bridge toward understanding the solution-state structure of the compounds, a key target in our research.

The crystalline state of the 1-hexadecyl-2,3-dimethylimidazolium ([C_{16}dmim]) salts possess several similarities despite the different anion structures. For example, the three structures show that the H···H interactions from the alkyl chains are the dominant intermolecular interactions, excluding ion charges. Thus, the arrangement of these hydrophobic domains is important to forming the solid-state structure for this class of compounds as expected. Furthermore, the anions interact with the cationic head group for each compound, forming non-conventional hydrogen bonds[80] with the aromatic and methyl hydrogens on the ring, following established trends for ILs.

A key observation derived from the crystal structure analysis is that in [C_{16}dmim][Br], π–π stacking of the cations is observed. While no π–π stacking is seen in [C_{16}dmim][I], a significant percentage of H···π interactions arising from adjacent methyl groups is observed. For [C_{16}dmim][NTf_2], however, neither stacking nor H···π interactions are noted, with the compound instead heavily favoring the formation of anion···π interactions instead. Thus, halide···π interactions appear to be less favored than NTf_2···π interactions. These different interactions within the crystals are reflected in distinct long-range ordering for the compounds. However, as expected, alkyl–alkyl stacking was a major driving force for the formation of the crystalline state.

UV-vis absorption studies were conducted on the four compounds to determine any changes in the solution-state ordering of the ILs to draw a connection between the solid-state structures and the interactions present in the solution. Several key observations connected the crystal and solution states for these compounds. First, the anion size correlated with different assemblies in the solution. This tracks with the crystal structures as each showed distinct cation–cation and cation–anion interactions, leading to unique structures. Second, characteristic anion$\cdots\pi$ absorption bands are observed in [C_{16}dmim][NTf_2] which were noted in the spectra of [C_{16}dmim][Cl] but not in the bromide nor iodide samples. Speculatively, this would suggest that Cl$\cdots\pi$ interactions should be present in the solid state of [C_{16}dmim][Cl], although no crystal of this compound was obtained. Finally, multiple assemblies of [C_{16}dmim][I] were observed in solution. This, in part, could explain the observed thermal data for [C_{16}dmim][I], wherein multiple solid–solid phase transitions were observed. Thus, our study of [C_{16}dmim]-based ILs helped solidify several theories concerning the link between intermolecular forces and their presence in the solution state of these compounds.

Our groups have also begun to look beyond the use of imidazole groups with respect to the synthesis and design of novel ILs.[81] Of particular interest to the present article is our study of thiazolium-based ILs.[82] In brief, the thiazolium ILs with long alkyl chains displayed comparable phase transitions, when compared to the imidazolium congeners. This observation was unexpected given the asymmetry of the cationic heterocycles. Furthermore, higher than anticipated enthalpies of crystallization were observed for these compounds, which prompted us to delve into exploring the solid-state structure of these compounds. To help rationalize these observations, several derivatives of the compounds were crystallized.

With respect to long-alkyl chain derivatives, [C_{16}-Thia][NTf_2] displayed the expected characteristics of ILs: dominant alkyl–alkyl interactions, π interactions with the heterocyclic cation, and a higher percentage of H-bonding with the anion (Fig. 11). Thus, given the predictable nature of these findings from this study, no overt signs were pointing to an explanation of the uncharacteristic melting points or energetics of the phase transitions. However, modern computers have allowed access to new software capable of delving deeper into the realm of non-covalent interactions, particularly when dealing with crystal structures. Notably, Hirshfeld surface analysis[83,84] has, for our group, become a fundamental tool in exploring the structure and interactions of ILs.

Analysis of the thiazolium-based ILs revealed the presence of σ-holes on the sulfur moiety of the heterocycle. In brief, these σ-holes are positively charged regions arising from the anisotropic distribution of electrons around an atom. Abundant literature is available that delves into far more detail than we are able to herein.[85] The inclusion of the sulfur moiety thus introduces additional cation–anion interactions in the form of S$\cdots$O and S$\cdots$Br interactions within the thiazolium-based ILs. These interactions are theorized to contribute to the distinct thermal properties of the ILs.

Thus, several important lessons were learned from this study and our other studies with respect to crystallography and ILs. First, crystallographic analysis can help shed light on the properties directly influenced by the structure of the ILs. As in our study on the [C_{16}dmim] compounds, correlations between the solid state and the solution state of the ILs are possible, offering tremendous insight into the structure–property relationships of long-alkyl chain ILs. Second, the inclusion of heteroatoms (sulfur or oxygen) or functional groups (alkenes) into the structure of an IL imparts more than simple geometric

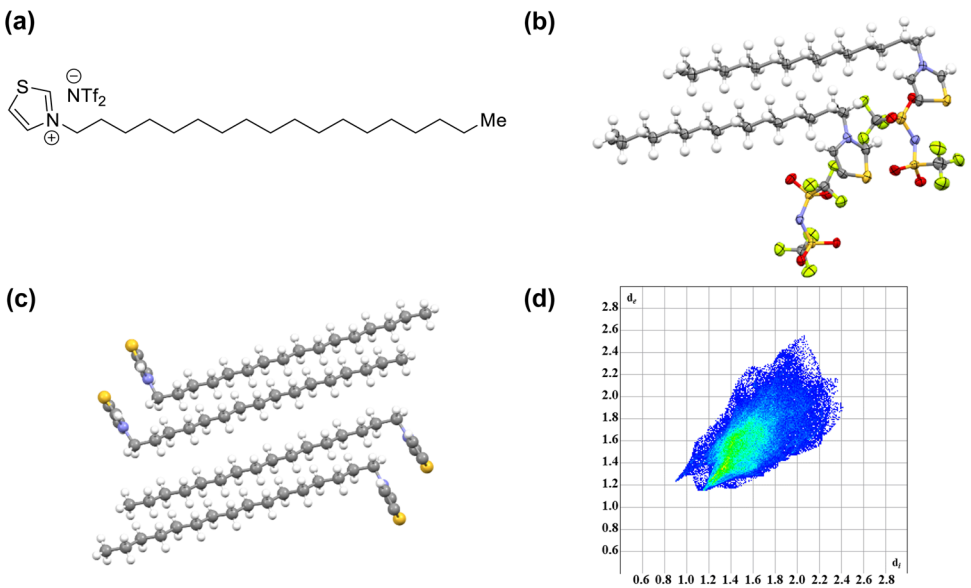

Fig. 11 Structure and asymmetric unit of [C_{16}-Thia][NTf_2] (a and b). Packing diagram of [C_{16}-Thia][NTf_2] showing alkyl–alkyl stacking (c). Interaction fingerprint of [C_{16}-Thia][NTf_2] showing a large percentage of H$\cdots$H interactions (green portion) (d). Reprinted with from ref. 82 with permission from the Elsevier.

changes (chain kinks). These functional groups also bring other key properties: chemical stability, changes in polarity, and new non-covalent interactions. Finally, as our groups become more adept at growing crystals of these systems, we can begin to validate and prove several aspects of our chain-kink theory. We hope these data will be part of the ongoing driving force for the continued study of these systems, leading to new insights and theories to develop the next generation of lipophilic ILs.

6. Applications of lipid-like ILs

The inclusion of sufficiently long alkyl chains imparts nonpolar characteristics to the lipid-like ILs, enabling their utilization in processes that involve nonpolar species that are not presently possible with traditional ILs. For example, the West group reported the higher solubility of ethane and ethylene as nonpolar gases in [oleyl-mim][NTf_2] (**5-AL**) than in conventional ILs.[86] Consistent with recent reports on other ILs characterized by substantial nonpolar content, the solubility of ethane is slightly higher than that of ethylene, in contrast to the relative solubility observed in traditional ILs with higher polarity. Likewise, the same laboratory has measured the solubility of CO_2 and N_2O in **5-AL** at various temperatures as a function of pressure up to *ca.* 2 MPa.[87] Data indicate that the ILs have a higher similarity to olive oil in terms of CO_2/N_2O solubility than the shorter-chain [$C_n$mim][NTf_2] ILs. These research studies provide evidence that these ILs show "nonpolar-like" solvent properties and have the potential to be used as substitutes for reactions and separation processes that currently depend on volatile, nonpolar solvents.

Additionally, Nan *et al.* reported the use of lipid-like ILs containing double bonds, thioether, and cyclopropyl moieties as stationary phases in two-dimensional gas chromatography (GC × GC) for separating aliphatic hydrocarbons in kerosene.[88] They reported comprehensive investigations into the correlation between IL structures and resulting solvation characteristics. The results were particularly encouraging for the separation of nonpolar components at high operating temperatures. The unique solvation properties of the ILs, such as their long alkyl chains and low melting points, contribute to their potential for providing unique selectivity and wide operating ranges when used as stationary phases in GC. The palmitoleyl IL (**2-AL**) demonstrated the highest level of selectivity towards nonpolar aliphatic hydrocarbons among the lipidic ILs examined in the study, as well as the commercial SUPELCOWAX 10 column. Moreover, among the lipidic ILs that were evaluated, the cyclopropanated IL **5-CP** not only proved to be a useful stationary phase for separation but also exhibited superior thermal stability compared to all other lipidic ILs in that role.

O'Brien *et al.* reported the synthesis of novel tetra(4-thiaalkyl)ammonium bromides *via* the thiol–ene reaction with the alkyl groups being dodecyl, tetradecyl, and octadecyl groups.[89] These long-chain quaternary ammonium salts were used as phase-transfer catalysts (PTCs) for the nucleophilic substitution of cyanide for bromide. Although 4-thiaalkylammonium salts exhibited slower reaction rates than their traditional quaternary counterparts, they still served as effective catalysts for transferring the nucleophile from the aqueous phase to the organic phase. In addition, we reported the facile synthesis of a library of trimethoxysilyl-functionalized lipid-like ILs with C_7–C_{15} thioether side chains using thiol–ene chemistry (Fig. 2).[42] They were found to be active surface coating agents by immobilizing them on magnetite supermagnetic Fe_3O_4 nanoparticles (SPNs), leading to the formation of novel ionogels. Notably, the particle size and particle loading exhibited considerable dependence on the tail lengths with higher side chain length resulting in higher particle loading. The variability in loading can be attributed to the differences in the interactions between the lipid-like ILs and the oleate moiety on the SPNs.

In our quest for safe and effective synthetic DNA delivery vectors, we employed thiol–yne chemistry to develop ammonium- and imidazolium-based lipid-like ILs with C_{12} and C_{14} saturated tails for DNA delivery (Fig. 7).[45] We observed that the ILs with imidazolium headgroups showed greater transfection efficacy than ammonium analogues. These compounds formed well-packed lamellar structures, which enhanced the stability of lipoplexes. Furthermore, substituting glycerol with a more lipophilic thioether backbone expanded the hydrophobic domain and moved the polar/nonpolar boundary to the level of the headgroup, ultimately improving the self-assembly. To further extend the hydrophobic domain, we developed a series of lipid-like ILs where myristyl and palmityl alkyl chains were directly attached to the methimazole ring through a one-step *N*,*S*-dialkylation reaction (Fig. 8).[54] The restrictive conformational freedom of the cationic headgroup was expected to confer an elongated linear shape, allowing for more compact packing along with increased self-assembly into lamellar phases (Fig. 8c). Remarkably, the extended charge delocalization throughout the cation resulted in increased hydrophobicity of the nonpolar domain, improving the self-assembling ability of the amphiphiles compared to ammonium cations. We demonstrated the efficacy of these materials in the condensation and release of plasmid DNA *in vitro* into HEK 293T cells, an epithelial line derived from human kidney tissue.

As part of our continuous efforts to design amphiphilic ILs with lipid characteristics for use as gene delivery vectors, our focus shifted towards creating ILs that exhibit enhanced fluidity and chemical stability while preserving their inherent lipophilic properties. To achieve these goals, we developed a strategy involving the dialkylation of 2-mercaptothiazole, utilizing saturated and *cis*-unsaturated C_{16} and C_{18} tails.[90] Surprisingly, he single crystal study showed the presence of a saturated 1-bromoalkane molecule co-crystallized with 2-mercaptothiazolium-based ILs through a host–guest co-crystallization effect, which was packed similarly to lipid-like bilayers (Fig. 12). The extended alkyl chains, coupled with σ-hole interactions strategically positioned by sulfur moieties, synergistically contributed to the crystallization of alkyl bromides. The transition from serendipity to a rational design strategy indicates how crystal engineering can be employed to achieve suitable systems for specific target-oriented tasks. The unique structures of the host–guest complexes exhibit similarities with biomembranes, opening avenues for exploration of the IL

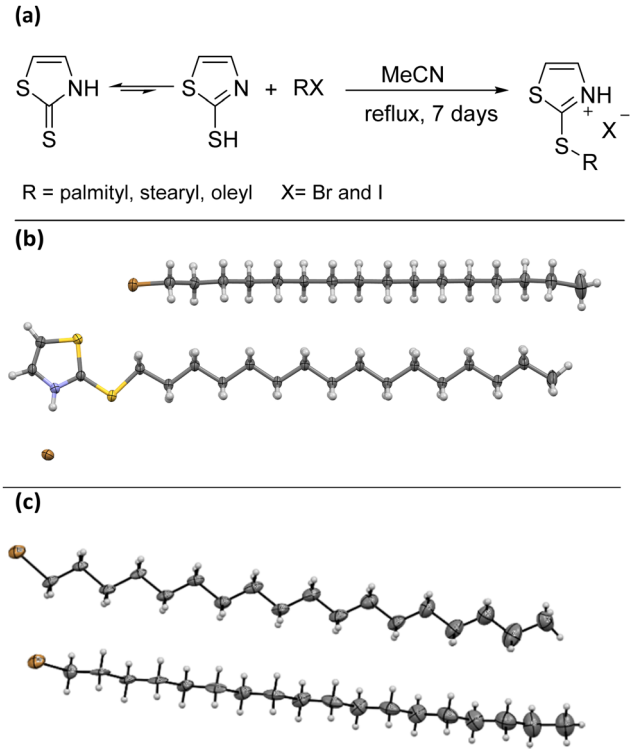

Fig. 12 (a) The serendipitous discovery of an ionic cocrystallization system using 2-mercaptothiazolium-based lipid-like ILs, leading to the first report of crystal structures of long-chain 1-bromoalkanes. Asymmetric units of the IL crystallized with 1-bromohexadecane (b) and 1-bromooctadecane (c) shown with 50% probability ellipsoids. Reprinted with from ref. 90 with permission from the Royal Society of Chemistry.

supramolecular chemistry and paving the way for designing customized materials with potential applications in the crystallography of Langmuir monolayers. Haloalkanes are high-value raw materials in the petrochemical industry and play a crucial role as intermediates in synthetic chemistry. They are typically produced through direct halogenation of alkanes and alkenes, leading to various structural and geometrical isomers. The separation process for these isomers is both energy-intensive and environmentally concerning. Therefore, this study presents innovative organic materials with the potential for the effective and sustainable separation of 1-bromoalkanes through crystallization.

7. Conclusion and future prospective

Similar to biomembranes, 1-*n*-alkyl-3-methylimidazolium ILs with long alkyl chains form polar and nonpolar nanodomains in the liquid state, corresponding to the charged polar region consisting of cationic head groups and anions and aggregated long nonpolar tails. These molecules show a high degree of self-organization, mobility, and hydrophobicity, which increased significantly with the elongation of the alkyl side chains. However, as the number of carbon atoms in the *n*-alkyl side chain increased above seven carbons ($n > 7$), their T_m values increased drastically. After this point, further elongation leads to a sharp uptick in T_m that quickly grows to exceed the ambient temperature, ultimately generating room-temperature solids – limiting the applicability of ILs in chemical reactions and separation processes. However, this dilemma can now be circumvented as it has been shown recently that lipid-like ILs (imidazolium salts with tails up to twenty carbons in length) can exhibit sub-ambient values of T_m as long as these aliphatic chains include olefin, thioether, and cyclopropyl moieties. Remarkably, clear and explicable correlations between T_m values and the nature of each functionalized alkyl chain are apparent, providing key insights into the structural features consistent with ILs that are simultaneously lipophilic and low-melting. As we learn more about structure–property relationships in lipid-like ILs, it should be increasingly straightforward to execute coordinated ion modifications that bring about desired changes in select physical properties (*e.g.*, T_m values in relatively narrow and specific ranges) while minimizing changes to others.

When it comes to IL design, the importance of reaction efficiency and facile chemistry cannot be overemphasized. These factors play a crucial role in the initial planning and creation of ILs, allowing the development of novel functional materials with significant applications. Click chemistry can overcome the synthetic hurdles associated with IL synthesis and facilitate the implementation of new ideas, thereby fostering advancements in the field and broadening the scope of structural possibilities for chemists. We anticipate that the efficiency and robustness of click reactions will continue to enable the development of novel functional IL materials with significant commercial applications.

Notwithstanding the abundant published papers, we still consider the field of lipid-like ILs as an emerging discipline with considerable prospects in creating novel solvents/materials with intriguing properties and functions. Apart from us, several other laboratories are engaged in the exploration of lipidic ionic materials, contributing to a broader understanding of lipidic IL platforms for diverse applications. Some of these applications include lipid-based formulations using lipophilic salt/IL forms for drug delivery[91] as well as utilization of long *n*-alkane/IL microdroplet platforms as acid catalysts.[92,93] Although these IL systems have already contributed to the introduction of interesting properties, key concerns such as biocompatibility (toxicity and biodegradation), longevity, and cost still need to be fine-tuned. The modern lipid-like IL field is characterized by an increasing emphasis on identifying specific design elements to create lipophilic, low-melting, and bio-innocuous ILs for specific tasks.

The use of machine learning (ML) models in developing ILs provides comprehensive insight into the physicochemical characteristics of IL families, enabling the identification of ILs with low T_m, high biocompatibility, and enhanced hydrophobicity.[94,95] This involves the prediction of the presence of symmetry-breaking functional groups that significantly influence their fluidity. By leveraging ML, we aim to accurately predict the physical and chemical properties of lipidic ILs while minimizing the cost and duration required to experimentally test different combinations of ions, paving the way for the discovery of tailor-made lipid-like ILs for a specific task. Supposedly, approximately 10^{18} anion–cation

interactions exist that can potentially lead to useful novel ILs.[1] However, designing lipid-like ILs with complex structures and diverse physicochemical properties is a challenging task. As a result, predictive computational tools such as artificial intelligence (AI) and ML are necessary to assist in the rational design and identifying symmetry-breaking moieties with desirable properties like practically low T_m, viscosity, ionic conductivity, and ecotoxicity. These tools also aid in examining mixtures' efficacy through advanced statistical learning methods using available quantitative structure–property/structure–activity relationship datasets from studies. With the exponential growth of data available in the literature, the use of statistical machine-learning algorithms to predict various physicochemical properties of lipophilic ILs is certainly a timely approach.

As a final note, we have provided an outlook into what may be possible in the future with ionic amphiphiles, emphasizing that these examples are merely the tip of the iceberg. We encourage others to embrace the utilization of these newly described families of ILs and explore their potential for various practical applications. In addition, we found the click approach to be highly advantageous as it makes IL synthesis more enjoyable and accessible. We hope that readers of this feature article will experience the same sense of joy.

Author contributions

John Yeboah, conceptualization (supporting), writing – original draft (supporting), writing – review & editing (supporting); Zachary Metott writing – original draft (supporting), writing – review & editing (supporting); Christopher M. Butch writing – review & editing (supporting); Patrick C. Hillesheim conceptualization (supporting), investigation (equal), writing – original draft (equal), writing review & editing (equal), funding acquisition (supporting); Arsalan Mirjafari conceptualization (lead), data curation (lead), funding acquisition (lead), supervision (lead), writing-original draft (lead), writing – review & editing (lead). The manuscript was written through contributions from all authors. All authors have given approval to the final version of the manuscript.

Conflicts of interest

There are no conflicts to declare.

Acknowledgements

Above all we thank and express our sincere gratitude to Professors Jim Davis, Rick O'Brien, and Kevin West at the University of South Alabama for their valuable research results, helpful discussions, and generous advice that inspired and informed us. A. M. is grateful to Dr Nicole Mirjafari for her meticulous proofreading of the manuscript, which significantly contributed to enhancing its quality and clarity. We thank Mr Muhammad Musozoda for his valuable assistance. This work is supported by the National Institute of General Medical Sciences of the National Institutes of Health (R21GM142011, R15GM153057), National Science Foundation (CHE–2244980), and the American Chemical Society Petroleum Research Fund (66195-UNI10). A. M. would like to thank Richard S. Shineman Foundation and the Oswego College Foundation for helping to make possible his current tenure at SUNY Oswego.

References

1 M. Deetlefs, M. Fanselow and K. R. Seddon, *RSC Adv.*, 2016, **6**, 4280–4288.
2 D. R. MacFarlane, M. Kar and J. M. Pringle, *Fundamentals of Ionic Liquids: From Chemistry to Applications*, Wiley-VCH Verlag GmbH & Co. KGaA, 2017.
3 *Commercial Applications of Ionic Liquids*, ed. M. B. Shiflett, Springer International Publishing, 2020.
4 A. J. Greer, J. Jacquemin and C. Hardacre, *Molecules*, 2020, **25**, 5207.
5 M. J. Earle, J. M. S. S. Esperança, M. A. Gilea, J. N. Canongia Lopes, L. P. N. Rebelo, J. W. Magee, K. R. Seddon and J. A. Widegren, *Nature*, 2006, **439**, 831–834.
6 J. H. Davis Jr., *Chem. Lett.*, 2004, **33**, 1072–1077.
7 T. L. Greaves and C. J. Drummond, *Chem. Soc. Rev.*, 2013, **42**, 1096–1120.
8 T. L. Greaves and C. J. Drummond, *Chem. Soc. Rev.*, 2008, **37**, 1709–1726.
9 B. Fernández-Castro, T. Méndez-Morales, J. Carrete, E. Fazer, O. Cabeza, J. R. Rodríguez, M. Turmine and L. M. Varela, *J. Phys. Chem. B*, 2011, **115**, 8145–8154.
10 R. Hayes, G. G. Warr and R. Atkin, *Chem. Rev.*, 2015, **115**, 6357–6426.
11 J. N. Canongia Lopes, M. F. Costa Gomes and A. A. H. Pádua, *J. Phys. Chem. B*, 2006, **110**, 16816–16818.
12 Y. Wang and G. A. Voth, *J. Am. Chem. Soc.*, 2005, **127**, 12192–12193.
13 J. N. A. Canongia Lopes and A. A. H. Pádua, *J. Phys. Chem. B*, 2006, **110**, 3330–3335.
14 X. Mao, P. Brown, C. Červinka, G. Hazell, H. Li, Y. Ren, D. Chen, R. Atkin, J. Eastoe, I. Grillo, A. A. H. Padua, M. F. Costa Gomes and T. A. Hatton, *Nat. Mater.*, 2019, **18**, 1350–1357.
15 A. A. H. Pádua and J. N. A. C. Lopes, *Ionic Liquids IV*, American Chemical Society, 2007, vol. 975, pp. 86–101.
16 C. Reichardt, *Green Chem.*, 2005, **7**, 339–351.
17 B. R. Mellein, S. N. V. K. Aki, R. L. Ladewski and J. F. Brennecke, *J. Phys. Chem. B*, 2007, **111**, 131–138.
18 J. P. Hallett and T. Welton, *ECS Trans.*, 2009, **16**, 33.
19 S. M. Murray, R. A. O'Brien, K. M. Mattson, C. Ceccarelli, R. E. Sykora, K. N. West and J. H. Davis, *Angew. Chem., Int. Ed.*, 2010, **49**, 2755–2758.
20 S. J. Singer and G. L. Nicolson, *Science*, 1972, **175**, 720–731.
21 I. López-Martin, E. Burello, P. N. Davey, K. R. Seddon and G. Rothenberg, *ChemPhysChem*, 2007, **8**, 690–695.
22 D. J. Siegel, G. I. Anderson, N. Cyr, D. S. Lambrecht, M. Zeller, P. C. Hillesheim and A. Mirjafari, *New J. Chem.*, 2021, **45**, 2443–2452.
23 T. Ichikawa, T. Kato and H. Ohno, *Chem. Commun.*, 2019, **55**, 8205–8214.
24 S. Zhang, J. Zhang, Y. Zhang and Y. Deng, *Chem. Rev.*, 2017, **117**, 6755–6833.
25 N. K. Kahlon, C. C. Weber, N. K. Kahlon and C. C. Weber, *Aust. J. Chem.*, 2021, **75**, 9–23.
26 G. G. Warr and R. Atkin, *Curr. Opin. Colloid Interface Sci.*, 2020, **45**, 83–96.
27 J. B. Marlow, R. Atkin and G. G. Warr, *J. Phys. Chem. B*, 2023, **127**, 1490–1498.
28 A. Mirjafari, R. A. O'Brien, S. M. Murray, K. M. Mattson, N. Mobarrez, K. N. West and J. H. Davis, in *ACS Symposium Series*, ed. A. E. Visser, N. J. Bridges and R. D. Rogers, American Chemical Society, Washington, DC, 2012, vol. 1117, pp. 199–216.
29 R. A. O'Brien, A. Mirjafari, K. M. Mattson, S. M. Murray, N. Mobarrez, E. A. Salter, A. Wierzbicki, J. H. Davis and K. N. West, *J. Phys. Chem. B*, 2014, **118**, 10232–10239.
30 R. A. O'Brien, P. C. Hillesheim, M. Soltani, K. J. Badilla-Nunez, B. Siu, M. Musozoda, K. N. West, J. H. Davis and A. Mirjafari, *J. Phys. Chem. B*, 2023, **127**, 1429–1442.

31 A. Mirjafari, R. A. O'Brien, K. N. West and J. H. Davis, *Chem. - Eur. J.*, 2014, **20**, 7576–7580.
32 M.-L. Kwan, A. Mirjafari, J. R. McCabe, R. A. O'Brien, D. F. Essi, L. Baum, K. N. West and J. H. Davis, *Tetrahedron Lett.*, 2013, **54**, 12–14.
33 B. D. Rabideau, M. Soltani, R. A. Parker, B. Siu, E. A. Salter, A. Wierzbicki, K. N. West and J. H. Davis, *Phys. Chem. Chem. Phys.*, 2020, **22**, 12301–12311.
34 G. I. Anderson, D. Hardy, P. C. Hillesheim, D. V. Wagle, M. Zeller, G. A. Baker and A. Mirjafari, *ACS Phys. Chem. Au*, 2023, **3**, 94–106.
35 J. K. Shah and E. J. Maginn, *Fluid Phase Equilib.*, 2010, **294**, 197–205.
36 J. De Roche, C. M. Gordon, C. T. Imrie, M. D. Ingram, A. R. Kennedy, F. Lo Celso and A. Triolo, *Chem. Mater.*, 2003, **15**, 3089–3097.
37 S. M. Murray, T. K. Zimlich, A. Mirjafari, R. A. O'Brien, J. H. Jr. Davis and K. N. West, *J. Chem. Eng. Data*, 2013, **58**, 1516–1522.
38 A. Mirjafari, S. M. Murray, R. A. O'Brien, A. C. Stenson, K. N. West and J. H. Davis, *Chem. Commun.*, 2012, **48**, 7522–7524.
39 H. C. Kolb, M. G. Finn and K. B. Sharpless, *Angew. Chem., Int. Ed.*, 2001, **40**, 2004–2021.
40 A. Mirjafari, *Chem. Commun.*, 2018, **54**, 2944–2961.
41 B. D. Fairbanks, L. J. Macdougall, S. Mavila, J. Sinha, B. E. Kirkpatrick, K. S. Anseth and C. N. Bowman, *Chem. Rev.*, 2021, **121**, 6915–6990.
42 M. Sanchez Zayas, J. C. Gaitor, S. T. Nestor, S. Minkowicz, Y. Sheng and A. Mirjafari, *Green Chem.*, 2016, **18**, 2443–2452.
43 M. Sanchez Zayas, S. Nestor, J. Gaitor, M. Reardon and A. Mirjafari, *ECS Trans.*, 2016, **75**, 191–198.
44 A. S. Thigpen, S. T. Nestor, R. A. O'Brien, S. Minkowicz, Y. Sheng, J. H. Davis, K. N. West and A. Mirjafari, *New J. Chem.*, 2017, **41**, 1625–1630.
45 J. C. Gaitor, L. M. Paul, M. M. Reardon, T. Hmissa, S. Minkowicz, M. Regner, Y. Sheng, S. F. Michael, S. Isern and A. Mirjafari, *Chem. Commun.*, 2017, **53**, 8328–8331.
46 R. D. Burton, D. J. Siegel, J. E. Muller, M. Regner, Y. Sheng, G. J. McManus, J. H. MacDonald and A. Mirjafari, *J. Mol. Liq.*, 2019, **296**, 111758.
47 R. A. O'Brien, A. Mirjafari, V. Jajam, E. N. Capley, A. C. Stenson, K. N. West and J. H. Davis, *Tetrahedron Lett.*, 2011, **52**, 5173–5175.
48 H. Lu, J. C. Wojtowicz and I. A. Butovich, *Chem. Phys. Lipids*, 2013, **170–171**, 55–64.
49 R. A. O'Brien, M. S. Zayas, S. T. Nestor, J. C. Gaitor, L. M. Paul, F. A. Edhegard, S. Minkowicz, R. E. Sykora, Y. Sheng, S. F. Michael, S. Isern and A. Mirjafari, *New J. Chem.*, 2016, **40**, 7795–7803.
50 A. N. Romeo and S. G. Običan, *Birth Defects Res.*, 2020, **112**, 1150–1170.
51 Y. Rong, A. Al-Harbi, B. Kriegel and G. Parkin, *Inorg. Chem.*, 2013, **52**, 7172–7182.
52 J. C. Gaitor, M. S. Zayas, D. J. Myrthil, F. White, J. M. Hendrich, R. E. Sykora, R. A. O'Brien, J. T. Reilly and A. Mirjafari, *Acta Crystallogr., Sect. E: Crystallogr. Commun.*, 2015, **71**, o1008–o1009.
53 F. Philippi and T. Welton, *Phys. Chem. Chem. Phys.*, 2021, **23**, 6993–7021.
54 D. J. Siegel, G. I. Anderson, L. M. Paul, P. J. Seibert, P. C. Hillesheim, Y. Sheng, M. Zeller, A. Taubert, P. Werner, C. Balischewski, S. F. Michael and A. Mirjafari, *ACS Appl. Bio Mater.*, 2021, **4**, 4737–4743.
55 S. Inuki and Y. Fujimoto, *Tetrahedron Lett.*, 2019, **60**, 1083–1090.
56 D. Poger and A. E. Mark, *J. Phys. Chem. B*, 2015, **119**, 5487–5495.
57 D. W. Grogan and J. E. Cronan, *Microbiol. Mol. Biol. Rev.*, 1997, **61**, 429–441.
58 M. S. Glickman, J. S. Cox and W. R. Jacobs, *Mol. Cell*, 2000, **5**, 717–727.
59 V. Rao, F. Gao, B. Chen, W. R. Jacobs and M. S. Glickman, *J. Clin. Invest.*, 2006, **116**, 1660–1667.
60 P. Cruz-Morales, K. Yin, A. Landera, J. R. Cort, R. P. Young, J. E. Kyle, R. Bertrand, A. T. Iavarone, S. Acharya, A. Cowan, Y. Chen, J. W. Gin, C. D. Scown, C. J. Petzold, C. Araujo-Barcelos, E. Sundstrom, A. George, Y. Liu, S. Klass, A. A. Nava and J. D. Keasling, *Joule*, 2022, **6**, 1590–1605.
61 V. H. Paschoal, L. F. O. Faria and M. C. C. Ribeiro, *Chem. Rev.*, 2017, **117**, 7053–7112.
62 G. Saielli, *Adv. Theory Simul.*, 2018, **1**, 1800084.
63 E. Bodo, *J. Phys. Chem. B*, 2022, **126**, 3–13.
64 E. Zorębski, M. Geppert-Rybczyńska and M. Zorębski, *J. Phys. Chem. B*, 2013, **117**, 3867–3876.
65 S. Galli, *J. Chem. Educ.*, 2014, **91**, 2009–2012.
66 J. C. Brooks-Bartlett and E. F. Garman, *Interdiscip. Sci. Rev.*, 2015, **40**, 244–264.
67 J. S. Wilkes and M. J. Zaworotko, *J. Chem. Soc., Chem. Commun.*, 1992, 965–967.
68 N. Winterton, *Ionic Liquids Completely UnCOILed*, John Wiley & Sons, Ltd, 2015, pp. 231–534.
69 J. D. Holbrey, W. M. Reichert, M. Nieuwenhuyzen, S. Johnson, K. R. Seddon and R. D. Rogers, *Chem. Commun.*, 2003, 1636.
70 S. Saouane, S. E. Norman, C. Hardacre and F. P. A. Fabbiani, *Chem. Sci.*, 2013, **4**, 1270.
71 A.-V. Mudring, *Aust. J. Chem.*, 2010, **63**, 544.
72 L. Gontrani, P. Ballirano, F. Leonelli and R. Caminiti, in *The Structure of Ionic Liquids*, ed. R. Caminiti and L. Gontrani, Springer International Publishing, Cham, 2014, pp. 1–37.
73 E. Brini, C. J. Fennell, M. Fernandez-Serra, B. Hribar-Lee, M. Lukšič and K. A. Dill, *Chem. Rev.*, 2017, **117**, 12385–12414.
74 J. N. A. Canongia Lopes and A. A. H. Pádua, *J. Phys. Chem. B*, 2006, **110**, 3330–3335.
75 H.-J. Schneider, *J. Phys. Org. Chem.*, 2022, **35**, e4340.
76 J. Dupont, *J. Braz. Chem. Soc.*, 2004, **15**, 341–350.
77 A. A. H. Pádua, M. F. Costa Gomes and J. N. A. Canongia Lopes, *Acc. Chem. Res.*, 2007, **40**, 1087–1096.
78 P. M. Dean, J. Turanjanin, M. Yoshizawa-Fujita, D. R. MacFarlane and J. L. Scott, *Cryst. Growth Des.*, 2009, **9**, 1137–1145.
79 S. A. Bellia, M. Metzler, M. Huynh, M. Zeller, A. Mirjafari, P. Cohn and P. C. Hillesheim, *Soft Matter*, 2023, **19**, 749–765.
80 I. Alkorta, I. Rozas and J. Elguero, *Chem. Soc. Rev.*, 1998, **27**, 163–170.
81 B. O'Rourke, C. Lauderback, L. I. Teodoro, M. Grimm, M. Zeller, A. Mirjafari, G. L. Guillet and P. C. Hillesheim, *ACS Omega*, 2021, **6**, 32285–32296.
82 C. Castillo, E. Chenard, M. Zeller, N. Hatab, P. F. Fulvio and P. C. Hillesheim, *J. Mol. Liq.*, 2021, **327**, 114800.
83 M. A. Spackman and D. Jayatilaka, *CrystEngComm*, 2009, **11**, 19–32.
84 P. R. Spackman, M. J. Turner, J. J. McKinnon, S. K. Wolff, D. J. Grimwood, D. Jayatilaka and M. A. Spackman, *J. Appl. Crystallogr.*, 2021, **54**, 1006–1011.
85 P. Politzer, J. S. Murray and T. Clark, *Phys. Chem. Chem. Phys.*, 2013, **15**, 11178.
86 B. D. Green, R. A. O'Brien, J. H. Davis and K. N. West, *Ind. Eng. Chem. Res.*, 2015, **54**, 5165–5171.
87 J. V. Langham, R. A. O'Brien, J. H. Davis and K. N. West, *J. Phys. Chem. B*, 2016, **120**, 10524–10530.
88 H. Nan, C. Zhang, R. A. O'Brien, A. Benchea, J. H. Davis and J. L. Anderson, *J. Chromatogr. A*, 2017, **1481**, 127–136.
89 R. A. O'Brien, C. W. West, B. E. Hollingsworth, A. C. Stenson, C. B. Henderson, A. Mirjafari, N. Mobarrez, K. N. West, K. M. Mattson, E. A. Salter, A. Wierzbicki and J. H. Davis, *RSC Adv.*, 2013, **3**, 24612.
90 M. Musozoda, J. E. Muller, G. I. Anderson, M. Boucher, M. Zeller, C. C. Raymond, P. C. Hillesheim and A. Mirjafari, *Chem. Commun.*, 2024, **60**, 1723–1726.
91 H. D. Williams, L. Ford, A. Igonin, Z. Shan, P. Botti, M. M. Morgen, G. Hu, C. W. Pouton, P. J. Scammells, C. J. H. Porter and H. Benameur, *Adv. Drug Delivery Rev.*, 2019, **142**, 75–90.
92 R. Greco, V. Lloret, M. Á. Rivero-Crespo, A. Hirsch, A. Doménech-Carbó, G. Abellán and A. Leyva-Pérez, *JACS Au*, 2021, **1**, 786–794.
93 A. S. Kashin and V. P. Ananikov, *Angew. Chem., Int. Ed.*, 2021, **60**, 18926–18928.
94 S. Koutsoukos, F. Philippi, F. Malaret and T. Welton, *Chem. Sci.*, 2021, **12**, 6820–6843.
95 Z. Acar, P. Nguyen and C. K. Lau, *App. Sci.*, 2022, **12**, 2408.